

Outlier detection in non-elliptical data by kernel MRCD

Joachim Schreurs, Iwein Vranckx, Mia Hubert,
Johan A.K. Suykens, Peter J. Rousseeuw

KU Leuven, Belgium

March 29, 2021

Abstract

The minimum regularized covariance determinant method (MRCD) is a robust estimator for multivariate location and scatter, which detects outliers by fitting a robust covariance matrix to the data. Its regularization ensures that the covariance matrix is well-conditioned in any dimension. The MRCD assumes that the non-outlying observations are roughly elliptically distributed, but many datasets are not of that form. Moreover, the computation time of MRCD increases substantially when the number of variables goes up, and nowadays datasets with many variables are common. The proposed Kernel Minimum Regularized Covariance Determinant (KMRCD) estimator addresses both issues. It is not restricted to elliptical data because it implicitly computes the MRCD estimates in a kernel induced feature space. A fast algorithm is constructed that starts from kernel-based initial estimates and exploits the kernel trick to speed up the subsequent computations. Based on the KMRCD estimates, a rule is proposed to flag outliers. The KMRCD algorithm performs well in simulations, and is illustrated on real-life data.

Keywords: Anomaly detection, High dimensional data, Kernelization, Minimum covariance determinant. Regularization.

1 Introduction

The minimum covariance determinant (MCD) estimator introduced in [21, 22] is a robust estimator of multivariate location and covariance. It forms the basis of robust versions of multivariate techniques such as discriminant analysis, principal component analysis, factor analysis and multivariate regression, see e.g. [16, 15] for an overview. The basic MCD method is quite intuitive. Given a data matrix of n rows with p columns, the objective is to find $h < n$ observations whose sample covariance matrix has the lowest determinant. The MCD estimate of location is then the average of those h points, whereas the scatter estimate is a multiple of their covariance matrix. The MCD has good robustness properties. It has a high breakdown value, that is, it can withstand a substantial number of outliers.

The effect of a small number of potentially far outliers is measured by its influence function, which is bounded [5].

Computing the MCD was difficult at first but became faster with the algorithm of [26] and the deterministic algorithm DetMCD [17]. An algorithm for n in the millions was recently constructed [6]. But all algorithms for the original MCD require that the dimension p be lower than h in order to obtain an invertible covariance matrix. In fact it is recommended that $n > 5p$ in practice [26]. This restriction implies that the original MCD cannot be applied to datasets with more variables than cases, that are commonly found in spectroscopy and areas where sample acquisition is difficult or costly, e.g. in the field of omics data.

A solution to this problem was recently proposed in [3], which introduced the minimum regularized covariance determinant (MRCD) estimator. The scatter matrix of a subset of h observations is now a convex combination of its sample covariance matrix and a target matrix. This makes it possible to use the MRCD estimator when the dimension exceeds the subset size. But the computational complexity of MRCD still contains a term $O(p^3)$ from the covariance matrix inversion, which limits its use for high-dimensional data. Another restriction is the assumption that the non-outlying observations roughly follow an elliptical distribution.

To address both issues we propose a generalization of the MRCD which is defined in a kernel induced feature space \mathcal{F} , where the proposed estimator exploits the kernel trick: the $p \times p$ covariance matrix is not calculated explicitly but replaced by the calculation of a $n \times n$ centered kernel matrix, resulting in a computational speed-up in case $n \ll p$. Similar ideas can be found in the literature, see e.g. [10, 11] which kernelized the minimum volume ellipsoid [21, 22]. The results of the KMRC algorithm with the linear kernel $k(x, y) = x^\top y$ and radial basis function (RBF) kernel $k(x, y) = e^{-\|x-y\|^2/(2\sigma^2)}$ are shown in Figure 1. This example will be described in detail in Section 6.

The paper is organized as follows. Section 2 describes the MCD and MRCD estimators. Section 3 proposes the kernel MRCD method. Section 4 describes the kernel-based initial estimators used as well as a kernelized refinement procedure, and proves that the optimization in feature space is equivalent to an optimization in terms of kernel matrices. The simulation study in Section 5 confirms the robustness of the method as well as the improved computation speed when using a linear kernel. Section 6 illustrates KMRC on three datasets, and Section 7 concludes.

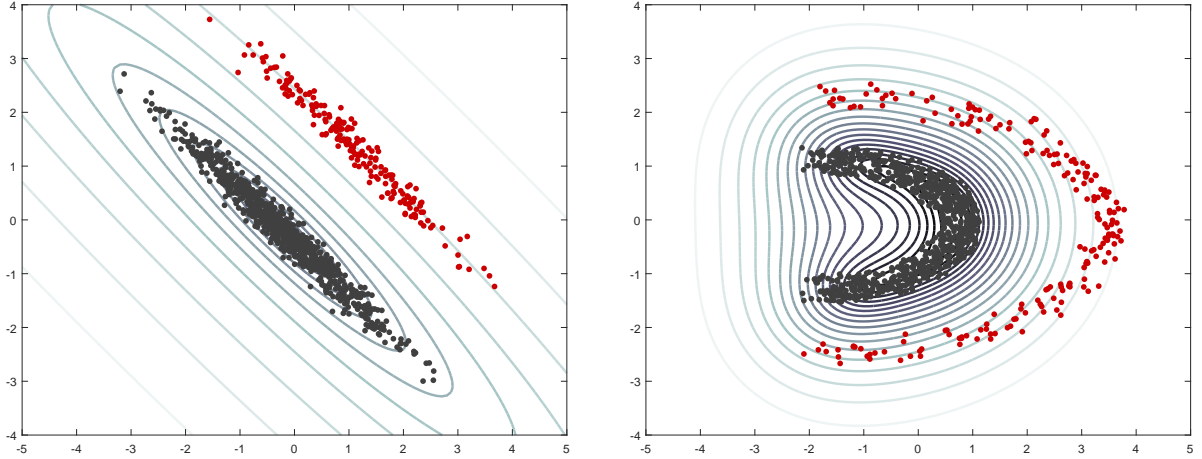


Figure 1: Illustration of kernel MRCD on two datasets of which the non-outlying part is elliptical (left) and non-elliptical (right). Both datasets contain 20% of outlying observations. The generated regular observations are shown in black and the outliers in red. In the panel on the left a linear kernel was used, and in the panel on the right a nonlinear kernel. The curves on the left are contours of the robust Mahalanobis distance in the original bivariate space. The contours on the right are based on the robust distance in the kernel-induced feature space.

2 The MCD and MRCD methods

2.1 The Minimum Covariance Determinant estimator

Assume that we have a p -variate dataset X containing n data points, where the i -th observation $x_i = (x_{i1}, x_{i2}, \dots, x_{ip})^\top$ is a p -dimensional column vector. We do not know in advance which of these points are outliers, and they can be located anywhere. The objective of the MCD method is to find a set H containing the indices of $|H| = h$ points whose sample covariance matrix has the lowest possible determinant. The user may specify any value of h with $n/2 \leq h < n$. The remaining $n - h$ observations could potentially be outliers. For each h -subset H the location estimate c^H is the average of these h points:

$$c^H = \frac{1}{h} \sum_{i \in H} x_i$$

whereas the scatter estimate is a multiple of their covariance matrix, namely

$$c_\alpha \hat{\Sigma}^H = \frac{c_\alpha}{h-1} \sum_{i \in H} (x_i - c^H)(x_i - c^H)^\top$$

where c_α is a consistency factor [5] that depends on the ratio $\alpha = h/n$. The MCD aims to minimize the determinant of $\hat{\Sigma}^H$ among all $H \in \mathcal{H}$, where the latter denotes the collection of all possible sets H with $|H| = h$:

$$\hat{\Sigma}_{\text{MCD}} = \underset{H \in \mathcal{H}}{\operatorname{argmin}} \det(\hat{\Sigma}^H). \quad (1)$$

Computing the exact MCD has combinatorial complexity, so it is infeasible for all but tiny datasets. However, the approximate algorithm FastMCD constructed in [26] is feasible.

FastMCD uses so-called concentration steps (C-steps) to minimize (1). Starting from any given $\hat{\Sigma}^H$, the C-step constructs a more concentrated approximation by calculating the Mahalanobis distance of every observation based on the location and scatter of the current subset H :

$$\text{MD}(x, c^H, \hat{\Sigma}^H) = \sqrt{(x - c^H)^\top (\hat{\Sigma}^H)^{-1} (x - c^H)}.$$

These distances are sorted and the h observations with the lowest $\text{MD}(x_i, c^H, \hat{\Sigma}^H)$ form the new h -subset, which is guaranteed to have an equal or lower determinant [26]. The C-step can be iterated until convergence.

2.2 The Minimum Regularized Covariance Determinant estimator

The minimum regularized covariance determinant estimator (MRCD) is a generalization of the MCD estimator to high dimensional data [3]. The MRCD subset H is defined by minimizing the determinant of the regularized covariance matrix $\hat{\Sigma}_{\text{reg}}^H$:

$$\hat{\Sigma}_{\text{MRCD}} = \underset{H \in \mathcal{H}}{\text{argmin}} \left(\det(\hat{\Sigma}_{\text{reg}}^H) \right),$$

where the regularized covariance matrix is given by

$$\hat{\Sigma}_{\text{reg}}^H = \rho T + (1 - \rho) c_\alpha \hat{\Sigma}^H$$

with $0 < \rho < 1$ and T a predetermined and well-conditioned symmetric and positive definite target matrix. The determination of ρ is done in a data-driven way such that $\hat{\Sigma}_{\text{MRCD}}$ has a condition number at most κ , for which [3] proposes $\kappa = 50$. The MRCD algorithm starts from six robust, well-conditioned initial estimates of location and scatter, taken from the DetMCD algorithm [17]. Each initial estimate is followed by concentration steps, and at the end the subset H with the lowest determinant is kept. Note that approximate algorithms like FastMCD and MRCD are much faster than exhaustive enumeration, but one can no longer formally prove a breakdown value. Fortunately, simulations confirm the high robustness of these methods. Also note that such approximate algorithms are guaranteed to converge, because they iterate C-steps starting from a finite number of initial fits. The algorithm may converge to a local minimum of the objective rather than its global minimum, but simulations have confirmed the accuracy of the result.

3 The Kernel MRCD Estimator

We now turn our attention to kernel transformations [28], formally defined as follows.

Definition 1. A function $k : \mathcal{X} \times \mathcal{X} \rightarrow \mathbb{R}$ is called a kernel on \mathcal{X} iff there exists a real Hilbert space \mathcal{F} and a map $\phi : \mathcal{X} \rightarrow \mathcal{F}$ such that for all x, y in \mathcal{X} :

$$k(x, y) = \langle \phi(x), \phi(y) \rangle,$$

where ϕ is called a feature map and \mathcal{F} is called a feature space.

We restrict ourselves to positive semidefinite (PSD) kernels. A symmetric function $k : \mathcal{X} \times \mathcal{X} \rightarrow \mathbb{R}$ is called PSD iff $\sum_{i=1}^n \sum_{j=1}^n c_i c_j k(x_i, x_j) \geq 0$ for any x_1, \dots, x_n in \mathcal{X} and any c_1, \dots, c_n in \mathbb{R} . Given an $n \times p$ dataset X , its kernel matrix is defined as $K = \Phi \Phi^\top$ with $\Phi = [\phi(x_1), \dots, \phi(x_n)]^\top$. The use of kernels makes it possible to operate in a high-dimensional, implicit feature space without computing the coordinates of the data in that space, but rather by replacing inner products by kernel matrix entries. A well known example is given by kernel PCA [27], where linear PCA is performed in a kernel-induced feature space \mathcal{F} instead of the original space \mathcal{X} . Working with kernel functions has the advantage that non-linear kernels enable the construction of non-linear models. Note that the size of the kernel matrix is $n \times n$, whereas the covariance matrix is $p \times p$. The latter is an advantage when dealing with datasets for which $n \ll p$, for then the memory and computational requirements are considerably lower.

Given an $n \times p$ dataset $X = \{x_1, \dots, x_n\}$ we thus get its image $\{\phi(x_1), \dots, \phi(x_n)\}$ in feature space, where it has the average

$$c_{\mathcal{F}} = \frac{1}{n} \sum_{i=1}^n \phi(x_i).$$

Note that the dimension of the feature space \mathcal{F} may be infinite. However, we will restrict ourselves to the subspace $\tilde{\mathcal{F}}$ spanned by $\{\phi(x_1) - c_{\mathcal{F}}, \dots, \phi(x_n) - c_{\mathcal{F}}\}$ so that $m := \dim(\tilde{\mathcal{F}}) \leq n - 1$. In this subspace the points $\phi(x_i) - c_{\mathcal{F}}$ thus have at most $n - 1$ coordinates. The covariance matrix in the feature space given by

$$\hat{\Sigma}_{\mathcal{F}} = \frac{1}{n-1} \sum_{i=1}^n (\phi(x_i) - c_{\mathcal{F}})(\phi(x_i) - c_{\mathcal{F}})^\top$$

is thus a matrix of size at most $(n-1) \times (n-1)$. Note that the covariance matrix is centered but the original kernel matrix is not. Therefore we construct the centered kernel matrix \tilde{K} by

$$\begin{aligned} \tilde{K}_{ij} &= \left(\phi(x_i) - \frac{1}{n} \sum_{\ell=1}^n \phi(x_\ell) \right)^\top \left(\phi(x_j) - \frac{1}{n} \sum_{\ell'=1}^n \phi(x_{\ell'}) \right) \\ &= K_{ij} - \frac{1}{n} \sum_{\ell=1}^n K_{\ell j} - \frac{1}{n} \sum_{\ell'=1}^n K_{i \ell'} + \frac{1}{n^2} \sum_{\ell=1}^n \sum_{\ell'=1}^n K_{\ell \ell'} \\ &= \left(K - \mathbf{1}_{nn} K - K \mathbf{1}_{nn} + \mathbf{1}_{nn} K \mathbf{1}_{nn} \right)_{ij} \end{aligned} \quad (2)$$

where $\mathbf{1}_{nn}$ is the $n \times n$ matrix with all entries set to $1/n$. Note that the centered kernel matrix is equal to $\tilde{K} = \tilde{\Phi} \tilde{\Phi}^\top$ with $\tilde{\Phi} = [\phi(x_1) - c_{\mathcal{F}}, \dots, \phi(x_n) - c_{\mathcal{F}}]^\top$ and is PSD by construction. The following result is due to [27].

Theorem 1. *Given an $n \times p$ dataset X , the sorted eigenvalues of the covariance matrix $\hat{\Sigma}_{\mathcal{F}}$ and those of the centered kernel matrix \tilde{K} satisfy*

$$\lambda_j^{\hat{\Sigma}_{\mathcal{F}}} = \frac{\lambda_j^{\tilde{K}}}{n-1}$$

for all $j = 1, \dots, m$ where $m = \text{rank}(\hat{\Sigma}_{\mathcal{F}})$.

Proof of Theorem 1. The eigendecomposition of the centered kernel matrix \tilde{K} is

$$\tilde{K} = \tilde{\Phi}\tilde{\Phi}^\top = V\Lambda V^\top$$

where $\Lambda = \text{diag}(\lambda_1, \dots, \lambda_n)$ with $\lambda_1 \geq \dots \geq \lambda_n$. The eigenvalue λ_j and eigenvector v_j satisfy

$$\tilde{\Phi}\tilde{\Phi}^\top v_j = \lambda_j v_j$$

for all $j = 1, \dots, m$. Multiplying both sides by $\tilde{\Phi}^\top/(n-1)$ gives

$$\left(\frac{1}{n-1}\tilde{\Phi}^\top\tilde{\Phi}\right)(\tilde{\Phi}^\top v_j) = \frac{\lambda_j}{n-1}(\tilde{\Phi}^\top v_j).$$

Combining the above equations results in

$$\hat{\Sigma}_{\mathcal{F}} v_j^{\hat{\Sigma}_{\mathcal{F}}} = \frac{\lambda_j}{n-1} v_j^{\hat{\Sigma}_{\mathcal{F}}}$$

for all $j = 1, \dots, m$ where $v_j^{\hat{\Sigma}_{\mathcal{F}}} = (\tilde{\Phi}^\top v_j)$ is the j -th eigenvector of $\hat{\Sigma}_{\mathcal{F}}$. The remaining eigenvalues of the covariance matrix, if any, are equal to zero. \square

The above result can be related to a representer theorem for kernel PCA [2]. It shows that the nonzero eigenvalues of the covariance matrix are proportional to the nonzero eigenvalues of the centered kernel matrix, thus proving that $\hat{\Sigma}_{\mathcal{F}}$ and \tilde{K} have the same rank.

What would a kernelized MCD estimator look like? It would have to be equivalent to applying the original MCD in the feature space, so that in case of the linear kernel the original MCD is obtained. The MCD estimate for location in the subspace $\tilde{\mathcal{F}}$ is

$$c_{\mathcal{F}}^H = \frac{1}{h} \sum_{i \in H} \phi(x_i)$$

whereas the covariance matrix now equals

$$\hat{\Sigma}_{\mathcal{F}}^H = \frac{1}{h-1} \sum_{i \in H} (\phi(x_i) - c_{\mathcal{F}}^H)(\phi(x_i) - c_{\mathcal{F}}^H)^\top.$$

Likewise, the robust distance becomes

$$\text{MD}(\phi(x), c_{\mathcal{F}}^H, \hat{\Sigma}_{\mathcal{F}}^H) = (\phi(x) - c_{\mathcal{F}}^H)^\top (\hat{\Sigma}_{\mathcal{F}}^H)^{-1} (\phi(x) - c_{\mathcal{F}}^H).$$

In these formulas the mapping function ϕ may not be known, but that is not necessary since we can apply the kernel trick. More importantly, the covariance matrix may not be invertible as the $\phi(x_i) - c_{\mathcal{F}}^H$ lie in a possibly high-dimensional space $\tilde{\mathcal{F}}$. We therefore propose to apply MRCD in $\tilde{\mathcal{F}}$ in order to make the covariance matrix invertible. Let $\tilde{\Phi}_H$ be the row-wise stacked matrix

$$\tilde{\Phi}_H = [\phi(x_{i(1)}) - c_{\mathcal{F}}^H, \dots, \phi(x_{i(h)}) - c_{\mathcal{F}}^H]^\top$$

where $i(1), \dots, i(h)$ are the indices in H . For any $0 < \rho < 1$ the regularized covariance matrix is defined as

$$\hat{\Sigma}_{\text{reg}}^H = (1 - \rho)\hat{\Sigma}_{\mathcal{F}}^H + \rho I_m = \frac{1 - \rho}{h - 1} \tilde{\Phi}_H^\top \tilde{\Phi}_H + \rho I_m$$

where I_m is the identity matrix in $\tilde{\mathcal{F}}$. The KMRCO method is then defined as

$$\hat{\Sigma}_{\text{KMRCO}} = \underset{H \in \mathcal{H}}{\operatorname{argmin}} \det(\hat{\Sigma}_{\text{reg}}^H) \quad (3)$$

where \mathcal{H} is the collection of subsets H of $\{1, \dots, n\}$ such that $|H| = h$ and $\hat{\Sigma}^H$ is of maximal rank, i.e. $\operatorname{rank}(\hat{\Sigma}^H) = \dim(\operatorname{span}(\phi(x_{i(1)}) - c_{\mathcal{F}}^H, \dots, \phi(x_{i(h)}) - c_{\mathcal{F}}^H)) = q$ with $q := \min(m, h - 1)$. We can equivalently say that the h -subset H is in general position. The corresponding regularized kernel matrix is

$$\tilde{K}_{\text{reg}}^H = (1 - \rho)\tilde{K}^H + (h - 1)\rho I_h \quad (4)$$

where $\tilde{K}^H = \tilde{\Phi}_H \tilde{\Phi}_H^T$ denotes the centered kernel matrix of h rows, that is, (2) with n replaced by h . The MRCO method in feature space $\tilde{\mathcal{F}}$ minimizes the determinant in (3) in $\tilde{\mathcal{F}}$. But we would like to carry out an optimization on kernel matrices instead. The following theorem shows that this is possible.

Theorem 2. *Minimizing $\det(\hat{\Sigma}_{\text{reg}}^H)$ over all subsets H in \mathcal{H} is equivalent to minimizing $\det(\tilde{K}_{\text{reg}}^H)$ over all h -subsets H with $\operatorname{rank}(\tilde{K}^H) = q$.*

Proof of Theorem 2. From Theorem 1 it follows that the nonzero eigenvalues of $\hat{\Sigma}_{\mathcal{F}}^H$ and \tilde{K}^H are related by $\lambda_j^{\hat{\Sigma}_{\mathcal{F}}^H} = \frac{1}{h-1}\lambda_j^{\tilde{K}^H}$. If H belongs to \mathcal{H} , $\hat{\Sigma}_{\mathcal{F}}^H$ has exactly q nonzero eigenvalues so \tilde{K}^H also has rank q , and vice versa. The remaining $m - q$ eigenvalues of $\hat{\Sigma}^H$ are zero, as well as the remaining $h - q$ eigenvalues of \tilde{K}^H . Now consider the regularized matrices

$$\hat{\Sigma}_{\text{reg}}^H = (1 - \rho)\hat{\Sigma}_{\mathcal{F}}^H + \rho I_m$$

and

$$\tilde{K}_{\text{reg}}^H = (1 - \rho)\tilde{K}^H + (h - 1)\rho I_h .$$

Computing the determinant of both matrices as a product of their eigenvalues yields:

$$\det(\hat{\Sigma}_{\text{reg}}^H) = \rho^{m-q} \prod_{j=1}^q ((1 - \rho)\lambda_j^{\hat{\Sigma}_{\mathcal{F}}^H} + \rho)$$

and

$$\begin{aligned} \det(\tilde{K}_{\text{reg}}^H) &= \rho^{h-q} \prod_{j=1}^q ((1 - \rho)\lambda_j^{\tilde{K}^H} + (h - 1)\rho) \\ &= \rho^{h-q} \prod_{j=1}^q (h - 1)((1 - \rho)\lambda_j^{\hat{\Sigma}_{\mathcal{F}}^H} + \rho) \\ &= \frac{\rho^{h-q}}{\rho^{m-q}} (h - 1)^q \det(\hat{\Sigma}_{\text{reg}}^H) . \end{aligned}$$

Therefore $\det(\tilde{K}_{\text{reg}}^H) = \rho^{h-m}(h-1)^q \det(\hat{\Sigma}_{\text{reg}}^H)$ in which the proportionality factor is constant, so the optimizations are equivalent. \square

Following [14] we can also express the robust Mahalanobis distance in terms of the regularized kernel matrix, by

$$\begin{aligned} \text{MD}(\phi(x), c_{\mathcal{F}}^H, \hat{\Sigma}_{\text{reg}}^H) &= \sqrt{(\phi(x) - c_{\mathcal{F}}^H)^\top (\hat{\Sigma}_{\text{reg}}^H)^{-1} (\phi(x) - c_{\mathcal{F}}^H)} \\ &= \sqrt{\frac{1}{\rho} \left(\tilde{k}(x, x) - (1 - \rho) \tilde{k}(H, x)^\top (\tilde{K}_{\text{reg}}^H)^{-1} \tilde{k}(H, x) \right)} \end{aligned} \quad (5)$$

where $\tilde{k}(x, x) = (\phi(x) - c_{\mathcal{F}}^H)^\top (\phi(x) - c_{\mathcal{F}}^H)$ is a special case of the formula $\tilde{k}(x, y) = k(x, y) - \sum_{i \in H} k(x_i, x) - \sum_{i \in H} k(x_i, y) + \sum_{i \in H} \sum_{j \in H} k(x_i, x_j)$ for $x = y$. The notation $\tilde{k}(H, x)$ stands for the column vector $\tilde{\Phi}_H(\phi(x) - c_{\mathcal{F}}^H) = [\tilde{k}(x_{i(1)}, x), \dots, \tilde{k}(x_{i(h)}, x)]^\top$ in which $i(1), \dots, i(h)$ are the members of H . This allows us to calculate the Mahalanobis distance in feature space from the kernel matrix, and consequently to perform the C-step procedure on it. Note that (5) requires inverting the matrix \tilde{K}_{reg}^H instead of the matrix $\hat{\Sigma}_{\text{reg}}^H$.

The C-step theorem of the MRCD in [3] shows that when you select a new h -subset as those i for which the Mahalanobis distance relative to the old h -subset is smallest, the regularized covariance determinant of the new h -subset is lower than or equal to that of the old one. In other words, C-steps lower the objective function of MRCD. Using Theorem 2, this C-step theorem thus also extends to the kernel MRCD estimator.

4 The Kernel MRCD Algorithm

This section introduces the elements of the kernel MRCD algorithm. If the original data comes in the form of an $n \times p$ dataset X , we start by robustly standardizing it. For this we first compute the univariate reweighted MCD estimator of [24] with coverage $h = \lfloor n/2 \rfloor + 1$ to obtain estimates of the location and scatter of each variable, which are then used to transform X to z -scores. The kernel matrix K is then computed from these z -scores. Note, however, that the data can come in the form of a kernel matrix that was not derived from data points with coordinates. For instance, a so-called string kernel can compute similarities between texts, such as emails, without any variables or measurements. Such a kernel basically compares the occurrence of strings of consecutive letters in each text. Since the KMRCD method does all its computations on the kernel matrix, it can also be applied to such data.

4.1 Initial estimates

The MRCD estimator needs initial h -subsets to start C-steps from. In the original FastMCD algorithm of [26] the initial h -subsets were obtained by drawing random $(p+1)$ -subsets out of the n data points. For each its empirical mean and covariance matrix were computed as well as the resulting Mahalanobis distances of all points, after which the subset with the h smallest distances was obtained. However, this procedure would not be possible in situations where $p > n$ because Mahalanobis distances require the covariance matrix to be invertible. The MRCD method instead starts from a small number of other initial estimators, inherited from the DetMCD algorithm in [17].

For the initial h -subsets in KMRCD we need methods that can be kernelized. We propose to use four such initial estimators, the combination of which has a good chance of

being robust against different contamination types. Since initial estimators can be inaccurate, a kernelized refinement step will be applied to each. We will describe these methods in turn.

The first initial method is based on the concept of spatial median. For data with coordinates, the spatial median is defined as the point m that has the lowest total Euclidean distance $\sum_i \|x_i - m\|$ to the data points. This notion also makes sense in the kernel context, since Euclidean distances in the feature space can be written in terms of the inner products that make up the kernel matrix. The spatial median in coordinate space is often computed by the Weiszfeld algorithm and its extensions, see e.g. [31]. A kernel algorithm for the spatial median was provided in [7]. It writes the spatial median $m_{\mathcal{F}}$ in feature space as a convex combination of the $\phi(x_i)$:

$$m_{\mathcal{F}} = \sum_{i=1}^n \gamma_i \phi(x_i)$$

in which the coefficients $\gamma_1, \dots, \gamma_n$ are unknown. The Euclidean distance of each observation to $m_{\mathcal{F}}$ is computed as the square root of

$$\begin{aligned} \|\phi(x_i) - m_{\mathcal{F}}\|^2 &= \|\phi(x_i) - \sum_{j=1}^n \gamma_j \phi(x_j)\|^2 \\ &= \|\phi(x_i)\|^2 + \|\sum_{j=1}^n \gamma_j \phi(x_j)\|^2 - 2\langle \phi(x_i), \sum_{j=1}^n \gamma_j \phi(x_j) \rangle \\ &= k(x_i, x_i) + \sum_{j=1}^n \sum_{\ell=1}^n \gamma_j \gamma_{\ell} k(x_j, x_{\ell}) - 2 \sum_{j=1}^n \gamma_j k(x_i, x_j) \end{aligned} \quad (6)$$

and the coefficients $\gamma_1, \dots, \gamma_n$ that minimize $\sum_i \|\phi(x_i) - m_{\mathcal{F}}\|$ are obtained by an iterative procedure described in Algorithm 2 in Section A.1 of the Supplementary Material. The first initial h -subset H is then given by the objects with the h lowest values of (6). Alternatively, H is described by a weight vector $w = (w_1, \dots, w_n)$ of length n , where

$$w_i := \begin{cases} 1 & \text{if } i \in H \\ 0 & \text{otherwise.} \end{cases} \quad (7)$$

The initial location estimate $c_{\mathcal{F}}$ in feature space is then the weighted mean

$$c_{\mathcal{F}} = \frac{\sum_{i=1}^n w_i \phi(x_i)}{\sum_{i=1}^n w_i}. \quad (8)$$

The initial covariance estimate $\hat{\Sigma}_{\mathcal{F}}$ is the weighted covariance matrix

$$\hat{\Sigma}_{\mathcal{F}} = \frac{1}{\sum_{i=1}^n w_i} \tilde{\Phi}^{\top} \text{diag}(u_1, \dots, u_n) \tilde{\Phi} \quad (9)$$

given by covariance weights (u_1, \dots, u_n) that in general may differ from the location weights (w_1, \dots, w_n) . But for the spatial median initial estimator one simply takes $u_i := w_i$ for all i .

The second initial estimator is based on the Stahel-Donoho outlyingness (SDO) of [29, 12]. In a space with coordinates it involves projecting the data points on many unit

length vectors (directions). We compute the kernelized SDO [9] of all observations and determine an h -subset as the indices of the h points with lowest outlyingness. This is then converted to weights w_i as in (7), and we put $u_i := w_i$ again. The entire procedure is listed as Algorithm 3 in the Supplementary Material.

The third initial h -subset is based on spatial ranks [8]. The spatial rank of $\phi(x_i)$ with respect to the other feature vectors is defined as:

$$\begin{aligned}
R_i &= \frac{1}{n} \left\| \sum_{j \neq i} \frac{\phi(x_i) - \phi(x_j)}{\|\phi(x_i) - \phi(x_j)\|} \right\| \\
&= \frac{1}{n} \left[\left(\sum_{j \neq i} \frac{\phi(x_i) - \phi(x_j)}{\|\phi(x_i) - \phi(x_j)\|} \right)^\top \left(\sum_{\ell \neq i} \frac{\phi(x_i) - \phi(x_\ell)}{\|\phi(x_i) - \phi(x_\ell)\|} \right) \right]^{\frac{1}{2}} \\
&= \frac{1}{n} \left[\sum_{j \neq i} \sum_{\ell \neq i} \frac{k(x_i, x_i) - k(x_i, x_j) - k(x_i, x_\ell) + k(x_j, x_\ell)}{\alpha(x_i, x_j)\alpha(x_i, x_\ell)} \right]^{\frac{1}{2}} \tag{10}
\end{aligned}$$

where $\alpha(x_i, x_j) = [k(x_i, x_i) + k(x_j, x_j) - 2k(x_i, x_j)]^{\frac{1}{2}}$. If R_i is large, this indicates that $\phi(x_i)$ lies further away from the bulk of the data than most other feature vectors. In this sense, the values R_i represent a different measure of the outlyingness of $\phi(x_i)$ in the feature space. We then consider the h lowest spatial ranks, yielding the location weights w_i by (7), and put $u_i := w_i$. The complete procedure is Algorithm 4 in the Supplementary Material. Note that this algorithm is closely related to the depth computation in [4] which appeared in the same year as [8].

The last initial estimator is a generalization of the spatial sign covariance matrix [32] (SSCM) to the feature space \mathcal{F} . For data with coordinates, one first computes the spatial median m described above. The SSCM then carries out a radial transform which moves all data points to a sphere around m , followed by computing the classical product moment of the transformed data:

$$\hat{\Sigma}^{\text{SSCM}} = \frac{1}{n-1} \sum_{i=1}^n \frac{(x_i - m)(x_i - m)^\top}{\|x_i - m\| \|x_i - m\|}.$$

The kernel spatial sign covariance matrix [7] is defined in the same way, by replacing x_i by $\phi(x_i)$ and m by $m_{\mathcal{F}} = \sum_{i=1}^n \gamma_i \phi(x_i)$. We now have two sets of weights. For location we use the weights $w_i = \gamma_i$ of the spatial median and apply (8). But for the covariance matrix we compute the weights $u_i = 1/\|\phi(x_i) - m_{\mathcal{F}}\|$ with the denominator given by (6). Next, we apply (9) with these u_i . The entire kernel SSCM procedure is listed as Algorithm 5 in the Supplementary Material. Note that kernel SSCM uses continuous weights instead of zero-one weights.

4.2 The refinement step

It happens that the eigenvalues of initial covariance estimators are inaccurate. In [18] this was addressed by re-estimating the eigenvalues, and [17] carried out this refinement step for all initial estimates used in that paper. In order to employ a refinement step in KMRCDC we need to be able to kernelize it. We will derive the equations for the general case of a location estimator given by a weighted sum (8) and a scatter matrix estimate given by a

weighted covariance matrix (9) so it can be applied to all four initial estimates. We proceed in four steps.

1. The first step consists of projecting the uncentered data on the eigenvectors $V_{\mathcal{F}}$ of the initial scatter estimate $\hat{\Sigma}_{\mathcal{F}}$:

$$B = \Phi V_{\mathcal{F}} = \Phi \tilde{\Phi}^{\top} D^{\frac{1}{2}} V = (K - K w 1_n^{\top}) D^{\frac{1}{2}} V, \quad (11)$$

where $D = \text{diag}(u_1, \dots, u_n) / (\sum_{i=1}^n u_i)$, $1_n = [1, \dots, 1]^{\top}$, and $V_{\mathcal{F}} = \tilde{\Phi}^{\top} D^{\frac{1}{2}} V$ with V the normalized eigenvectors of the weighted centered kernel matrix $\hat{K} = (D^{\frac{1}{2}} \tilde{\Phi})(D^{\frac{1}{2}} \tilde{\Phi})^{\top} = D^{\frac{1}{2}} \tilde{K} D^{\frac{1}{2}}$.

2. Next, the covariance matrix is re-estimated by

$$\Sigma_{\mathcal{F}}^* = V_{\mathcal{F}} L V_{\mathcal{F}}^{\top} = \tilde{\Phi}^{\top} D^{\frac{1}{2}} V L V^{\top} D^{\frac{1}{2}} \tilde{\Phi},$$

where $L = \text{diag}(Q_n^2(B_{.1}), \dots, Q_n^2(B_{.n}))$ in which Q_n is the scale estimator of Rousseeuw and Croux [23] and $B_{.j}$ is the j -th column of B .

3. The center is also re-estimated, by

$$c_{\mathcal{F}}^* = (\Sigma_{\mathcal{F}}^*)^{\frac{1}{2}} \text{median}(\Phi(\Sigma_{\mathcal{F}}^*)^{-\frac{1}{2}})$$

where median stands for the spatial median. This corresponds to using a modified feature map $\phi^*(x) = \phi(x)(\Sigma_{\mathcal{F}}^*)^{-\frac{1}{2}}$ for the spatial median or running Algorithm 2 with the modified kernel matrix

$$\begin{aligned} K^* &= \Phi \tilde{\Phi}^{\top} D^{\frac{1}{2}} V L^{-1} V^{\top} D^{\frac{1}{2}} \tilde{\Phi} \Phi^{\top} \\ &= (K - K w 1_n^{\top}) D^{\frac{1}{2}} V L^{-1} D^{\frac{1}{2}} (K - K w 1_n^{\top})^{\top}. \end{aligned} \quad (12)$$

Transforming the spatial median gives us the desired center:

$$c_{\mathcal{F}}^* = (\Sigma_{\mathcal{F}}^*)^{\frac{1}{2}} \sum_{i=1}^n (\Sigma_{\mathcal{F}}^*)^{-\frac{1}{2}} \gamma_i^* \phi(x_i) = \sum_{i=1}^n \gamma_i^* \phi(x_i),$$

where γ_i^* are the weights of the spatial median for the modified kernel matrix.

4. The kernel Mahalanobis distance is calculated as

$$\begin{aligned} d_{\mathcal{F}}^*(x) &= (\phi(x) - c_{\mathcal{F}}^*)^{\top} (\Sigma_{\mathcal{F}}^*)^{-1} (\phi(x) - c_{\mathcal{F}}^*) \\ &= (\phi(x) - c_{\mathcal{F}}^*)^{\top} \tilde{\Phi}^{\top} D^{\frac{1}{2}} V L^{-1} V^{\top} D^{\frac{1}{2}} \tilde{\Phi} (\phi(x) - c_{\mathcal{F}}^*) \\ &= k^*(x, X) D^{\frac{1}{2}} V L^{-1} V^{\top} D^{\frac{1}{2}} k^*(x, X)^{\top} \end{aligned} \quad (13)$$

with

$$\begin{aligned} k^*(x, X) &= k(x, X) - \sum_{i=1}^n w_i k(x, x_i) 1_n^{\top} \\ &\quad - \sum_{j=1}^n \gamma_j^* k(x_j, X) - \sum_{i=1}^n \sum_{j=1}^n w_i \gamma_j^* k(x_i, x_j) 1_n^{\top} \end{aligned}$$

where $k(x, X) = [k(x, x_1), \dots, k(x, x_n)]$.

The h points with the smallest $d_{\mathcal{F}}^*(x)$ form the refined h -subset. The entire procedure is Algorithm 6 in the Supplementary Material.

4.3 Kernel MRCD algorithm

We now have all the elements to compute the kernel MRCD by Algorithm 1. Given any PSD kernel matrix and subset size h , the algorithm starts by computing the four initial estimators described in Section 4.1. Each initial estimate is then refined according to Section 4.2. Next, kernel MRCD computes the regularization parameter ρ . This is done with a kernelized version of the procedure in [3]. For each initial estimate we choose ρ such that the regularized kernel matrix \tilde{K}_{reg}^H of (4) is well-conditioned. If we denote by λ the vector containing the eigenvalues of the centered kernel matrix \tilde{K}^H , the condition number of \tilde{K}_{reg}^H is

$$\kappa(\rho) = \frac{(h-1)\rho + (1-\rho)\max(\lambda)}{(h-1)\rho + (1-\rho)\min(\lambda)} \quad (14)$$

and we choose ρ such that $\kappa(\rho) \leq 50$. (Section A.3 in the supplementary material contains a simulation study supporting this choice.) Finally, kernel C-steps are applied until convergence, where we monitor the objective function of Section 3.

Algorithm 1 Kernel MRCD.

1. **Input:** kernel matrix K , subset size h .
 2. Compute the weights of the four initial estimates of location and scatter as in Section 4.1.
 3. Refine each initial estimate as in Section 4.2.
 4. For each resulting subset, determine $\rho^{(i)}$ such that $\kappa(\rho^{(i)}) \leq 50$.
 5. Determine the final ρ as in [3]: if $\max_i \rho^{(i)} \leq 0.1$ set $\rho = \max_i \rho^{(i)}$, otherwise set $\rho = \max(0.1, \text{median}_i(\rho^{(i)}))$.
 6. For $H = H^{(1)}, \dots, H^{(4)}$ perform C-steps as follows:
 - (a) Compute the regularized kernel matrix \tilde{K}_{reg}^H for the h -subset H from (4).
 - (b) Calculate the regularized Mahalanobis distance for each observation i by (5).
 - (c) Redefine H as the h indices i with smallest distance.
 - (d) Compute and store the objective. If not converged, go back to (a).
 7. Select the h -subset with the overall smallest objective function.
 8. **Output:** the final h -subset and the robust distances.
-

In the special case where the linear kernel is used, the centered kernel matrix \tilde{K}^H immediately yields the regularized covariance matrix $\hat{\Sigma}_{\text{reg}}^H$ through

$$\hat{\Sigma}_{\text{reg}}^H = \frac{1-\rho}{h-1} (\tilde{X}^H)^\top \tilde{V} \Lambda \tilde{V}^\top \tilde{X}^H + \rho I_h$$

where $\tilde{X}^H = X^H - \frac{1}{h} \sum_{i \in H} x_i$ is the centered matrix of the observations in H and Λ and \tilde{V} contain the eigenvalues and normalized eigenvectors of \tilde{K}^H . (The derivation is given in

Section A.2.) So instead of applying MRCD to coordinate data we can also run KMRCDC with a linear kernel and transform \hat{K}^H to $\hat{\Sigma}_{\text{reg}}^H$ afterward. This computation is faster when the data has more dimensions than cases.

4.4 Anomaly detection by KMRCDC

Mahalanobis distances (MD) relative to robust estimates of location and scatter are very useful to flag outliers, because outlying points i tend to have higher MD_i values. The standard way to detect outliers by means of the MCD in low dimensional data is to compare the robust distances to a cutoff that is the square root of a quantile of the chi-squared distribution with degrees of freedom equal to the data dimension [26]. However, in high dimensions the distribution of the squared robust distances is no longer approximately chi-squared, which makes it harder to determine a suitable cutoff value. Faced with a similar problem [25] introduced a different approach, based on the empirical observation that robust distances of the non-outliers in higher dimensional data tend to have a distribution that is roughly similar to a lognormal. They first transform the distances MD_i to $\text{LD}_i = \log(0.1 + \text{MD}_i)$, where the term 0.1 prevents numerical problems should a (near-)zero MD_i occur. The location and spread of the non-outlying LD_i are then estimated by $\hat{\mu}_{\text{MCD}}$ and $\hat{\sigma}_{\text{MCD}}$, the results of applying the univariate MCD to all LD_i using the same h as in the KMRCDC method itself. Data point i is then flagged iff

$$\frac{\text{LD}_i - \hat{\mu}_{\text{MCD}}(\text{LD})}{\hat{\sigma}_{\text{MCD}}(\text{LD})} > z(0.995)$$

where $z(0.995)$ is the 0.995 quantile of the standard normal distribution. The cutoff value for the untransformed robust distances is thus

$$c = \exp(\hat{\mu}_{\text{MCD}}(\text{LD}) + z(0.995)\hat{\sigma}_{\text{MCD}}(\text{LD})) - 0.1 . \quad (15)$$

The user may want to try different values of h to be used in both the KMRCDC method itself as well as in the $\hat{\mu}_{\text{MCD}}$ and $\hat{\sigma}_{\text{MCD}}$ in (15). One typically starts with a rather low value of h , say $h = 0.5n$ when the linear kernel is used and there are up to 10 dimensions, and $h = 0.75n$ in all other situations. This will provide an idea about the number of outliers in the data, after which it is recommended to choose h as high as possible provided $n - h$ exceeds the number of outliers. This will improve the accuracy of the estimates.

4.5 Choice of bandwidth

A commonly used kernel function is the radial basis function (RBF) $k(x, y) = e^{-\|x-y\|^2/(2\sigma^2)}$ which contains a tuning constant σ that needs to be chosen. When the downstream learning task is classification σ is commonly selected by cross validation, where it is assumed that the data has no outliers or they have already been removed. However, in our unsupervised outlier detection context there is nothing to cross validate. Therefore, we will use the so-called median heuristic [13] given by

$$\sigma^2 = \text{median}\{\|x_i - x_j\|^2 ; 1 \leq i < j \leq n\} \quad (16)$$

in which the x_i are the standardized data in the original space. We will use this σ in all our examples.

4.6 Illustration on toy examples

We illustrate the proposed KMRCO method on the two toy examples in Figure 1. Both datasets consist of $n = 1000$ bivariate observations. The elliptical dataset in the left panel was generated from a bivariate Gaussian distribution, plus 20% of outliers. The non-elliptical dataset in the panel on the right is frequently used to demonstrate kernel methods [30]. This dataset also contains 20% of outliers, which are shown in red and form the outer curved shape. We first apply the non-kernel MCO method, which does not transform the data, with $h = \lfloor 0.75n \rfloor$. (Not using a kernel is equivalent to using the linear kernel.) The results are in Figure 2. In the panel on the left this works well because the MCO method was developed for data of which the majority has a roughly elliptical shape. For the same reason it does not work well on the non-elliptical data in the right hand panel.

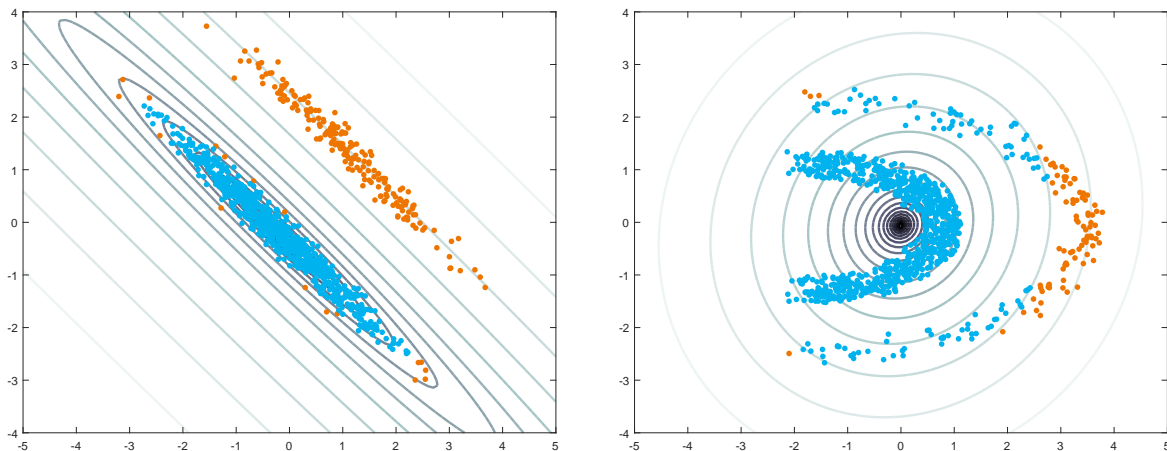
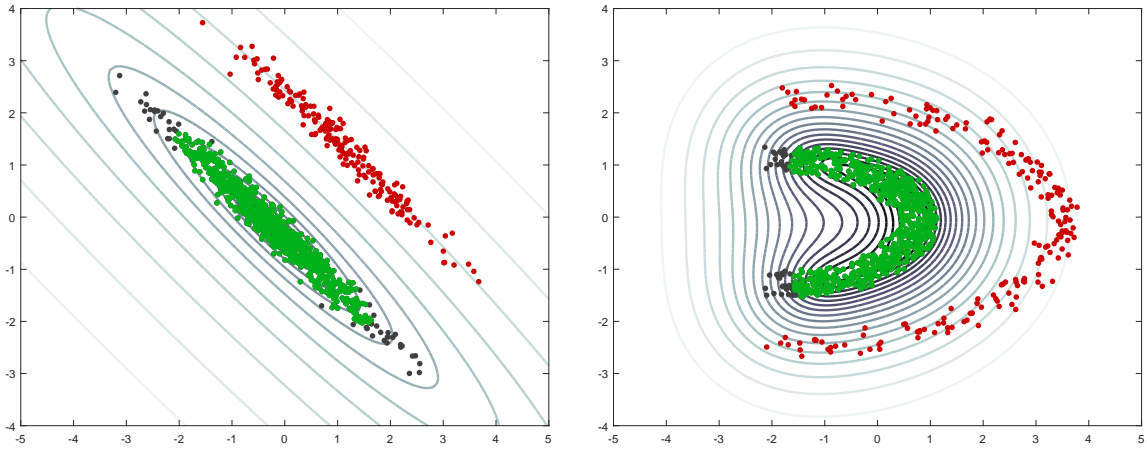


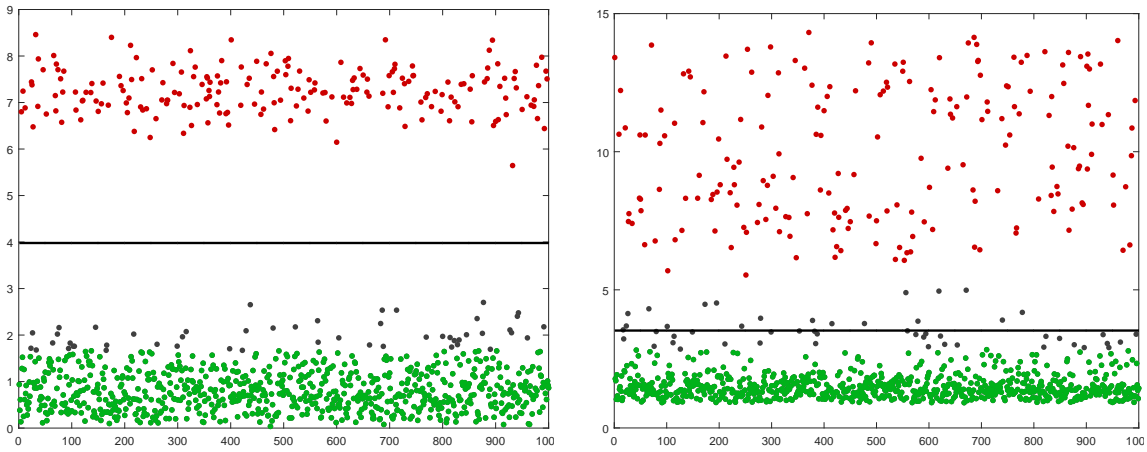
Figure 2: Results of the non-kernel MCO method on the toy datasets of Figure 1. The contour lines are level curves of the MCO-based Mahalanobis distance.

We now apply the kernel MRCO method to the same datasets. For the elliptical dataset we use the linear kernel, and for the non-elliptical dataset we use the RBF kernel with tuning constant σ given by formula (16). This yields Figure 3. We first focus on the left hand column. The figure shows three stages of the KMRCO runs. At the top, in Figure 3(a), we see the result for the selected h -subset, after the C-steps have converged. The members of that h -subset are the green points, whereas the points generated as outliers are colored red. Since h is lower than the true number of inlying points, some inliers (shown in black) are not included in the h -subset. In the next step, Figure 3(b) shows the robust Mahalanobis distances, with the horizontal line at the cutoff value given by formula (15). The final output of KMRCO shown in Figure 3(c) has the flagged outliers in orange and the points considered inliers in blue. As expected, this result is similar to that of the non-kernel MCO in the left panel of Figure 2.

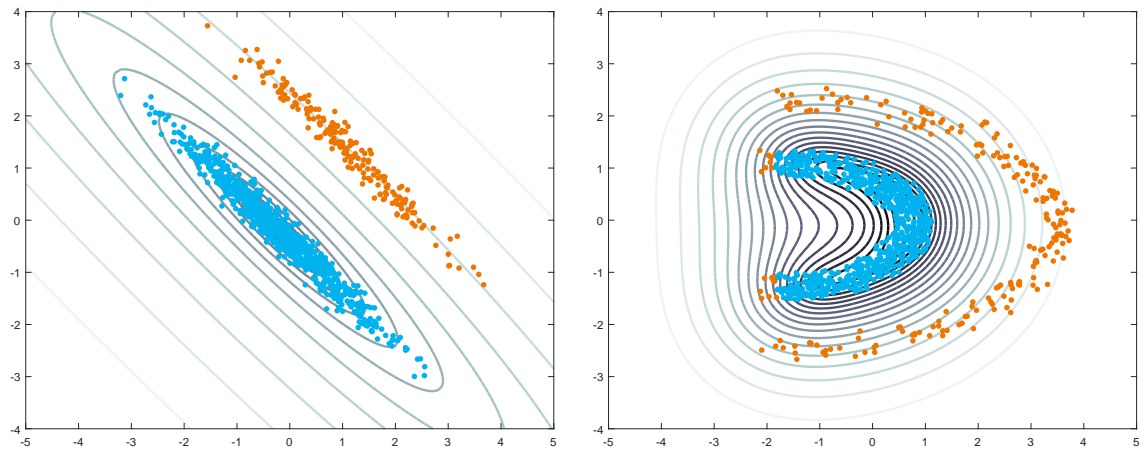
The right hand column of Figure 3 shows the stages of the KMRCO run on the non-elliptical data. The results for the selected h -subset in Figure 3(a) look much better than in the right hand panel of Figure 2, because the level curves of the robust distance now follow the shape of the data. In stage (b) we see that the distances of the inliers and the outliers are fairly well separated by the cutoff (15), with a few borderline cases, and stage (c) is the final result. This illustrates that using a nonlinear kernel allows us to fit non-elliptical data.



(a) h -subset results after C -step convergence.



(b) Robust Mahalanobis distances with outlier cutoff.



(c) Final results with the flagged outliers shown in orange.

Figure 3: Kernel MRCD results on the toy datasets of Figure 1. In the left column the linear kernel was used, and in the right column the RBF kernel. The three stages (a), (b) and (c) are explained in the text.

5 Simulation Study

5.1 Simulation study with linear kernel

In this section we compare the KMRCO method proposed in the current paper, run with the linear kernel, to the MRCD estimator of Boudt et al. [3]. Recall that using the linear kernel $k(x, y) = x^\top y$ means that the feature space can be taken identical to the coordinate space, so using the linear kernel is equivalent to not using a kernel at all. Our purpose is twofold. First, we want to verify whether KMRCO performs well in terms of robustness and accuracy, and that its results are consistent with those of MRCD. And secondly, we wish to measure the computational speedup obtained by KMRCO in high dimensions. In order to obtain a fair comparison we run MRCD with the identity matrix as target, which corresponds to the target of KMRCO. All computations are done in MATLAB on a machine with Intel Core i7-8700K and 16 GB of 3.70GHz RAM.

For the uncontaminated data, that is, for contamination fraction $\varepsilon = 0$, we generate n cases from a p -variate normal distribution with true covariance matrix Σ . Since the methods under consideration are equivariant under translations and rescaling variables, we can assume without loss of generality that the center μ of the distribution is 0 and that the diagonal elements of Σ are all 1. We denote the distribution of the clean data by $\mathcal{N}(0, \Sigma)$. Since the methods are not equivariant to arbitrary nonsingular affine transformations we cannot set Σ equal to the identity matrix. Instead we consider Σ of the ALYZ type, generated as in Section 4 of [1], which yields a different Σ in each replication, but always with condition number 100. The main steps of the construction of Σ in [1] are the generation of a random orthogonal matrix to provide eigenvectors, and the generation of p eigenvalues such that the ratio between the largest and the smallest is 100, followed by iterations to turn the resulting covariance matrix into a correlation matrix while preserving the condition number. (In section A.3 of the supplementary material also Σ matrices with higher condition numbers were generated, with similar results.)

For a contamination fraction $\varepsilon > 0$ we replace a random subset of $\lfloor \varepsilon n \rfloor$ observations by outliers of different types. *Shift contamination* is generated from $\mathcal{N}(\mu_C, \Sigma)$ where μ_C lies in the direction where the outliers are hardest to detect, which is that of the last eigenvector v of the true covariance matrix Σ . We rescale v by making $v^\top \Sigma^{-1} v = E[Y^2] = p$ where $Y^2 \sim \chi_p^2$. The center is taken as $\mu_C = kv$ where we set $k = 200$. Next, *cluster contamination* stems from $\mathcal{N}(\mu_C, 0.05^2 I_p)$ where I_p is the identity matrix. Finally, *point contamination* places all outliers in the point μ_C so they behave like a tight cluster. These settings make the simulation consistent with those in [3, 17] and [6]. The deviation of an estimated scatter matrix $\hat{\Sigma}$ relative to the true covariance matrix Σ is measured by the Kullback–Leibler (KL) divergence $\text{KL}(\hat{\Sigma}, \Sigma) = \text{trace}(\hat{\Sigma}\Sigma^{-1}) - \log(\det(\hat{\Sigma}\Sigma^{-1})) - p$. The speedup factor is measured as $\text{speedup} = \text{time}(\text{MRCD})/\text{time}(\text{KMRCO})$. Different combinations of n and p are generated, ranging from $p = n/2$ to $p = 2n$.

Table 1 presents the Kullback–Leibler deviation results. The top panel is for $\varepsilon = 0$, the middle panel for $\varepsilon = 0.1$ and the bottom panel for $\varepsilon = 0.3$. All table entries are averages over 50 replications. First look at the results without contamination. By comparing the three choices for h , namely $\lfloor 0.5n \rfloor$, $\lfloor 0.75n \rfloor$ and $\lfloor 0.9n \rfloor$, we see that lowering h in this setting leads to increasingly inaccurate estimates $\hat{\Sigma}$. This is the price we pay for being more robust to outliers, since $n - h$ is an upper bound on the number of outliers the methods can handle. When we look at the panels for higher ε we see a similar pattern.

When $\varepsilon = 0.1$ the choice $\lfloor 0.9n \rfloor$ is sufficiently robust, and the lower choices of h have higher KL deviation. But when $\varepsilon = 0.3$ only the choice $h = \lfloor 0.5n \rfloor$ can detect the outliers, the other choices cause the estimates to break down. These patterns are confirmed by the averaged MSE $= \sum_{i=1}^p \sum_{j=1}^p (\hat{\Sigma} - \Sigma)_{ij}^2 / p^2$ shown in Table 7 in the Supplementary Material.

From these results we conclude that it is important that h be chosen lower than n minus the number of outliers, but not much lower since that would make the estimates less accurate. A good strategy is to first run with a low h , which reveals the number of outliers, and then to choose a higher h that can still handle the outliers and yields more accurate results as well.

As expected the KMRCDC results are similar to those of MRCD, but not identical because there are differences in the selection of initial estimators, also leading to differences in the resulting regularization parameter ρ shown in Table 8 in the Supplementary Material.

We now turn our attention to the computational speedup factors in Table 2, that were derived from the same simulation runs as Table 1. Overall KMRCDC ran substantially faster than MRCD, with the factor becoming larger when n decreases and/or the dimension p increases. There are two reasons for the speedup. First of all, the MRCD algorithm computes six initial scatter estimates, of which the last one is the most computationally demanding since it computes a robust bivariate correlation of every pair of variables, requiring $p(p-1)/2$ computations whose total time increases fast with p . Part of the speedup stems from the fact that KMRCDC does not use this initial estimator, whereas its own four kernelized initial estimates gave equally robust results. This explains most of the speedup in Table 2.

For $p > n$ there is a second reason for the speedup, the use of the kernel trick. In particular, each C-step requires the computation of the Mahalanobis distances of all cases. MRCD does this by inverting the $p \times p$ covariance matrix $\hat{\Sigma}_{\text{reg}}^H$, whereas KMRCDC uses equation (5) which implies that it suffices to invert the $n \times n$ kernel matrix \tilde{K}_{reg}^H , which takes time complexity $O(n^3)$ instead of $O(p^3)$.

5.2 Simulation with nonlinear kernel

In this section we compare the proposed KMRCDC estimator to the MRCD estimator of Boudt et al. [3] on two types of non-elliptical datasets. The first type is generated by a copula. We start by considering the t copula [20] with Pearson correlation 0.1 and $\nu = 1$ degrees of freedom. The black points in the left panel of Figure 4 were generated from this copula. We then added contamination in the form of uniformly distributed random noise on the unit square, where points lying close to the regular distribution were removed. The red points in the left panel of Figure 4 are the outliers. Apart from the t copula we also consider the Frank, Clayton, and Gumbel copulas with Kendall rank correlation $\tau = 0.6$. They are visualized in Figure 9 in section A.6 of the Supplementary Material.

The proposed estimator is also benchmarked in a second type of setting where the regular observations are uniformly distributed on the unit circle, and inside the circle are outliers generated from the Gaussian distribution with center 0 and covariance matrix equal to 0.04 times the identity matrix. This setting is illustrated in Figure 5. This is a simple example where the clean data lie near a manifold.

In the simulation we generated 100 datasets of each type, with $n = 500$ and the outlier fraction ε equal to 0.1 or 0.2, so the number of regular observations is $n(1 - \varepsilon)$. With all four copulas the KMRCDC estimator used the radial basis function with bandwidth (16).

Table 1: Kullback-Leibler deviations of $\hat{\Sigma}$ from Σ .

	Point contamination			Shift contamination			Cluster contamination		
	Value of h/n			Value of h/n			Value of h/n		
	0.50	0.75	0.90	0.50	0.75	0.90	0.50	0.75	0.90
$\varepsilon = 0 :$									
KMRCD									
400×200	126.72	80.03	64.65	127.66	78.99	64.54	129.37	79.42	64.45
300×200	174.37	110.03	88.43	176.46	108.45	87.94	174.52	109.68	87.50
200×200	262.41	171.74	140.18	263.03	172.23	140.66	260.21	169.02	140.45
200×300	492.70	381.13	319.42	491.65	379.07	317.45	491.64	373.38	319.44
200×400	724.41	602.78	535.59	715.59	602.44	532.55	731.76	607.21	537.27
MRCD									
400×200	126.58	80.82	65.65	127.00	79.99	65.63	128.92	80.63	65.35
300×200	175.88	110.57	89.49	176.21	109.22	88.79	174.36	110.28	88.85
200×200	265.04	174.13	141.23	264.57	173.56	141.10	261.93	172.00	141.05
200×300	499.11	384.91	323.48	500.80	383.02	322.14	499.30	378.74	324.27
200×400	734.47	608.04	539.54	729.52	610.79	539.24	738.21	611.83	543.84
$\varepsilon = 0.1 :$									
KMRCD									
400×200	128.14	78.48	63.16	127.28	78.28	62.28	128.91	79.75	62.71
300×200	176.76	107.10	86.94	174.32	109.86	87.37	176.13	108.54	87.86
200×200	263.76	172.21	137.31	260.06	171.46	137.72	260.42	171.76	136.27
200×300	493.36	368.80	311.48	488.10	377.46	311.04	491.24	378.81	319.45
200×400	728.07	600.12	558.79	723.40	596.87	535.08	720.44	604.06	534.81
MRCD									
400×200	128.22	79.59	64.19	127.92	79.76	63.48	129.09	81.11	63.91
300×200	174.17	107.67	88.05	172.96	111.15	88.00	173.46	109.50	89.12
200×200	262.71	171.55	137.51	259.52	170.79	138.03	261.48	170.95	136.31
200×300	493.66	368.88	309.88	494.44	382.69	312.85	499.27	382.10	320.48
200×400	723.42	599.88	525.99	736.52	601.15	536.73	733.36	611.43	537.56
$\varepsilon = 0.3 :$									
KMRCD									
400×200	127.46	4914.7	2073.9	126.26	1142.7	1613.4	124.73	1124.8	1600.6
300×200	176.51	5104.1	2046.1	176.82	1125.9	1597.6	173.30	1117.2	1555.3
200×200	257.91	5180.6	2038.3	255.55	1168.8	1559.1	257.90	1163.6	1535.9
200×300	485.71	5494.5	2230.0	488.19	1310.0	1626.8	490.05	1311.1	1616.9
200×400	714.57	5779.1	2316.1	721.41	1448.7	1736.7	718.17	1423.4	1721.1
MRCD									
400×200	124.33	6771.6	3082.7	125.15	1395.6	2068.9	124.68	1371.1	2078.5
300×200	164.89	7118.6	3049.4	172.11	1415.2	2076.5	168.51	1393.0	2011.1
200×200	237.08	7519.3	3075.1	241.27	1481.1	2040.1	242.59	1485.8	2014.7
200×300	450.12	8233.1	3413.4	483.07	1653.4	2122.5	483.67	1659.9	2102.4
200×400	663.35	8585.0	3507.7	717.65	1812.8	2212.9	719.74	1790.5	2201.6

Table 2: Speedup factors of KMRCO relative to MRCD.

	Point contamination			Shift contamination			Cluster contamination		
	Value of h/n			Value of h/n			Value of h/n		
	0.50	0.75	0.90	0.50	0.75	0.90	0.50	0.75	0.90
$\varepsilon = 0 :$									
400×200	97	95	89	99	96	91	100	98	92
300×200	281	242	229	281	242	229	284	242	228
200×200	301	249	227	299	253	226	301	253	228
200×300	661	558	516	623	562	519	657	563	520
200×400	1144	979	897	1157	982	892	1159	978	899
$\varepsilon = 0.1 :$									
400×200	98	90	87	96	92	89	96	92	90
300×200	263	227	211	278	240	225	282	239	224
200×200	292	243	216	302	252	225	302	249	228
200×300	631	534	504	652	564	516	664	567	512
200×400	1113	951	870	1157	981	902	1110	980	903
$\varepsilon = 0.3 :$									
400×200	77	79	72	100	96	93	99	95	93
300×200	211	193	185	281	251	233	288	251	234
200×200	234	206	202	301	262	238	299	257	238
200×300	543	472	432	653	564	522	654	566	520
200×400	1000	791	749	1161	976	911	1150	977	900

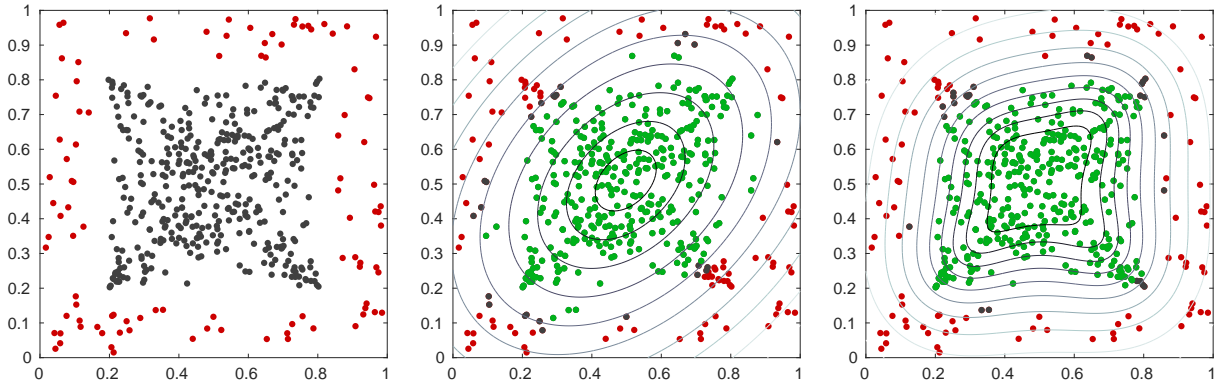


Figure 4: Illustration of the non-elliptical simulation setting with data generated from the t copula, plus 20% of outlying observations. In the left panel, the regular observations are shown in black and the outliers in red. The results of the MRCD estimator are in the middle panel, and those of the KMRCD estimator in the rightmost panel, each for $h = 0.75n$. In those panels the points in the h -subset are shown in green, and the other points with the $n(1 - \varepsilon)$ lowest (kernel) Mahalanobis distance are depicted in grey. The remaining points are shown in red. The curves are contours of the robust (kernel) Mahalanobis distance.

For the circle-based data the polynomial kernel $k(x, y) = (x^\top y + 1)^2$ of degree 2 was used.

We measure the performance by counting the number of outliers in the h -subset, and among the $n(1 - \varepsilon)$ points with the lowest (kernel) Mahalanobis distance. The averaged counts over the 100 replications are shown in Table 3. By comparing the rows of KMRCD and MRCD with the same ε , we see that MRCD has more true outliers in its h -subset and its $n(1 - \varepsilon)$ set. In the table, KMRCD outperforms MRCD for both choices of ε and for all three choices of h . The good performance of KMRCD is also seen in the right panel of Figure 4, where the contours of the kernel Mahalanobis distance nicely follow the distribution. The difference between MRCD and KMRCD is most apparent on the circle-based data: in Figure 5 the KMRCD fits the regular data on the circle, whereas the original MRCD method, by its nature, considers the outliers in the center as regular data.

We conclude that in this nonlinear setting, KMRCD has successfully extended the MRCD to non-elliptical distributions. We want to add two remarks about this. First, as in all kernel-based methods the choice of the kernel is important, and choosing a different kernel can lead to worse results. And second, just as in the linear setting h should be lower than n minus the number of outliers, so in practice it is recommended to first run with a low h , look at the results in order to find out how many outliers there are, and possibly run again with a higher h .

Section A.4 of the supplementary material contains additional simulation results about the computation time of the four initial estimators in KMRCD and their subsequent C-steps, in different settings with linear and nonlinear kernels.

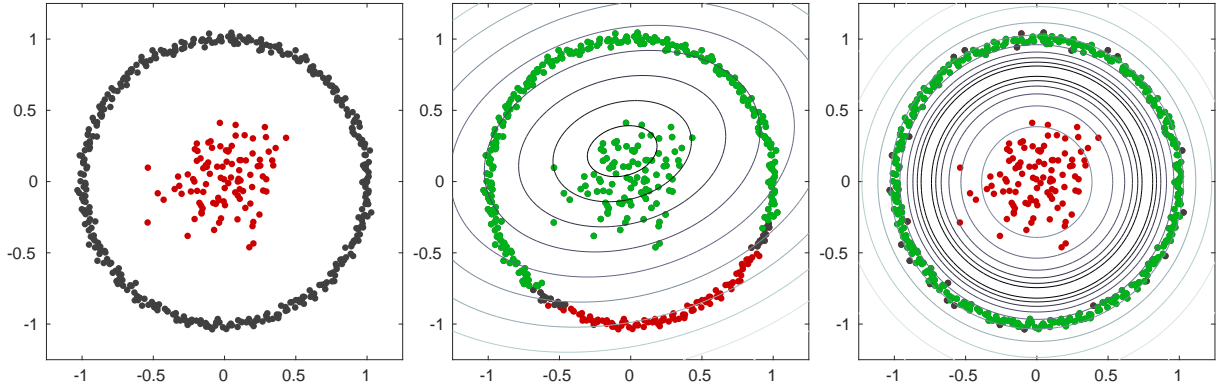


Figure 5: Illustration of the non-elliptical simulation setting with data generated from the circle manifold, plus 20% of outlying observations. The remainder of the description is as in Figure 4.

Table 3: Average number of outliers in the h -subset H , and among the $n(1 - \varepsilon)$ points with lowest (kernel) Mahalanobis distance.

	t copula			Frank copula			Clayton copula			Gumbel copula			Circle		
	0.75	0.8	0.9	0.75	0.8	0.9	0.75	0.8	0.9	0.75	0.8	0.9	0.75	0.8	0.9
$\varepsilon = 0.1$:															
KMRCD															
H	0	0	0.5	0	0	2.9	0	0	2.6	0	0	2.8	0	0	0
$n(1 - \varepsilon)$	10	8.2	0.5	3.9	4.2	2.9	4.3	4.4	2.6	4.4	4.7	2.8	0	0	0
MRCD															
H	1.2	2.9	13.3	1.3	2.1	11.2	2.4	3.7	11.6	2.0	2.9	11.2	50	50	50
$n(1 - \varepsilon)$	22.5	20.3	13.3	12.9	12.2	11.2	14.4	14.0	11.6	13.7	13.3	11.2	50	50	50
$\varepsilon = 0.2$:															
KMRCD															
H	0.1	2.1	/	0	3.5	/	0	3.3	/	0	3.8	/	0	0	/
$n(1 - \varepsilon)$	9.0	2.1	/	4.8	3.5	/	4.4	3.3	/	5.2	3.8	/	0	0	/
MRCD															
H	12.9	21.7	/	8.4	16.3	/	10.2	18.5	/	10	18.7	/	100	100	/
$n(1 - \varepsilon)$	27.5	21.7	/	18.9	16.3	/	19.7	18.5	/	20.1	18.7	/	100	100	/

6 Experiments

6.1 Food industry example

We now turn our attention to a real dataset from the food industry. In that setting datasets frequently contain outliers, because samples originate from natural products which are often contaminated by insect damage, local discolorations and foreign material. It also happens that the image acquisition signals yield non-elliptical data, and in that case a kernel transform can help.

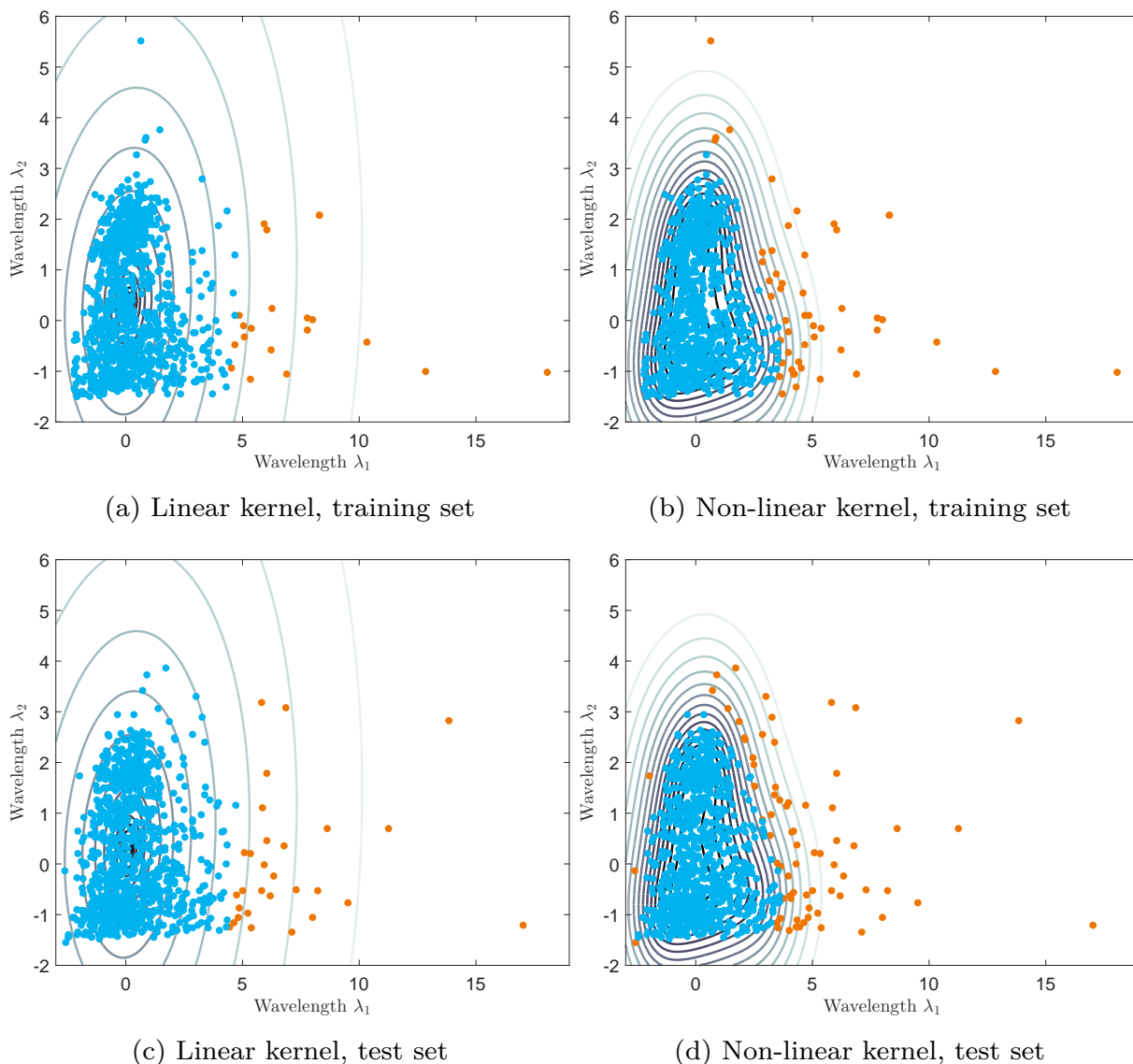


Figure 6: Food industry example: KMRCD results with the linear kernel (left column) and the RBF kernel (right column). The top row contains the training data, and the resulting fits were applied to the test data in the bottom row.

The dataset is bivariate and contains two color signals measured on organic sultana raisin samples. The goal is to classify these into inliers and outliers, so that during produc-

tion outliers can be physically removed from the product in real time. There are training data and test data, but the class label ‘outlier’ is not known beforehand. The scatter plot of the training data in Figure 6 (a) reveals the non-elliptical (and to some extent triangular) structure of the inliers. Three types of outliers are visible. Those with high values of λ_1 and low λ_2 at the bottom right correspond to foreign, cap-stem related material like wood, whereas points with high values of λ_2 represent discolorations. There are also a few points with high values of both λ_1 and λ_2 which correspond to either discolored raisins or objects with clear attachment points of cap-stems. Outliers of any of these three types need to be flagged and removed from the product. From manually analyzing data of this product it is known beforehand that the fraction of outliers is rather low, at most around 2%.

We first run KMRCDC on the training data. In its preprocessing step it standardizes both variables. For comparison purposes we use two kernels. In the left hand column of Figure 6 we apply the linear kernel, and in the right hand column we use the RBF kernel with tuning constant σ given by (16). Since we know the fraction of outliers is low we can put $h = \lfloor 0.95n \rfloor$. Each figure shows the flagged points in orange and the remaining points in blue, and the contour lines are level curves of the robust distance.

The fit with linear kernel in Figure 6 (a) has contour lines that do not follow the shape of the data very well, and as a consequence it fails to flag some of the outliers, such as those with high λ_2 and some with relatively high values of both λ_1 and λ_2 . The KMRCDC fit with nonlinear kernel in Figure 6 (b) has contour lines that model the data more realistically. This fit does flag all three types of outliers correctly. Both trained models were then used to classify the previously unseen test set. The results are similar to those on the training data. The anomaly detection with linear kernel in Figure 6 (c) again misses the raisin discolorations, which would keep these impurities in the final consumer product. Fortunately, the method with the nonlinear kernel in panel (d) does flag them.

6.2 MNIST digits data

Our last example is high dimensional. The MNIST dataset contains images of handwritten digits from 0 to 9, at the resolution of 28×28 grayscale pixels (so there are 784 dimensions), and was downloaded from <http://yann.lecun.com/exdb/mnist>. There is a training set and a test set. Both were subsampled to 1000 images. To the training data we added noise distributed as $\mathcal{N}(0, (0.5)^2)$ to 20% of the images, and in the test set we added noise with the same distribution to all images. We then applied KMRCDC with RBF kernel with tuning constant σ given by (16) and $h = \lfloor 0.75n \rfloor$ to the 1000 training images. Next, we computed the eigenvectors of the robustly estimated covariance matrix.

Our goal is to denoise the images in the test set by projecting them onto the main eigenvectors found in the training data. As we are interested in a reconstruction of the data in the original space rather than in the feature space, we transform the scores back to the original input space by the iterative optimization method of [19].

The top panel of Figure 7 illustrates what happens when applying this computation to the classical covariance matrix in feature space, which corresponds to classical kernel PCA [27]. The bottom panel is based on KMRCDC. The first row of each panel displays original test set images, and the second row shows the test images after the noise was added. The first and second rows do not depend on the estimation method, but the remaining rows do. There we see the results of projecting on the first 5, 15, and 30 eigenvectors of each method. In the top panel those images are rather diffuse, which indicates that the classical

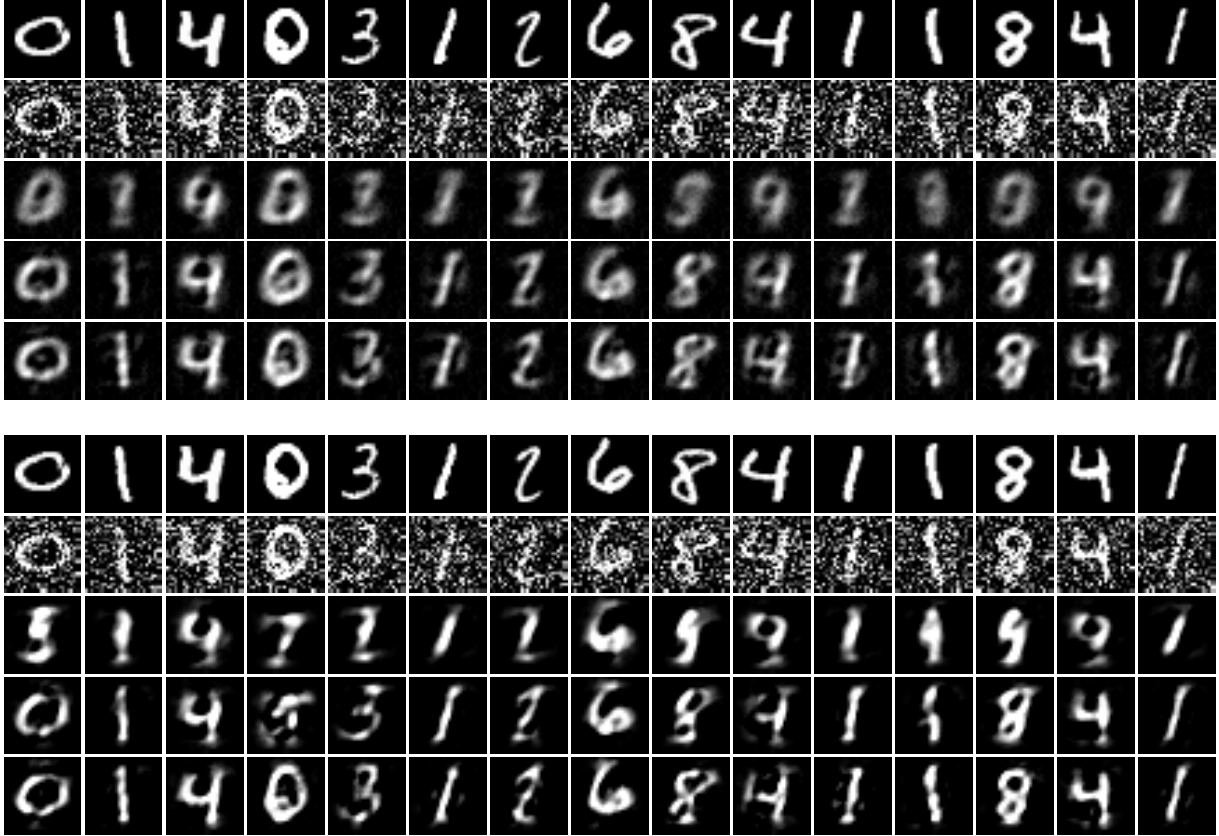


Figure 7: MNIST denoising results based on the classical covariance matrix (top panel) and on the KMRCD estimate (bottom panel). The first and second rows of each panel show the same original and noise-added test set images. The remaining rows contain the results of projecting on the first 5, 15, and 30 eigenvectors.

approach was affected by the training images with added noise and considers the added noise as part of its model. This implies that increasing the number of eigenvectors used will not improve the overall image quality much. The lower panel contains sharper images, because the robust fit of the training data was less affected by the images with added noise that acted as outliers.

We can also compute the mean absolute error $\sum_{i=1}^n \sum_{j=1}^p |x_{i,p} - \hat{x}_{i,p}| / (np)$ between the original test images (with $p = 784$ dimensions) and the projected versions of the test images with added noise. Figure 8 shows this deviation as a function of the number of eigenvectors used in the projection. The deviations of the robust method are systematically lower than those of the classical method, confirming the visual impression from Figure 7.

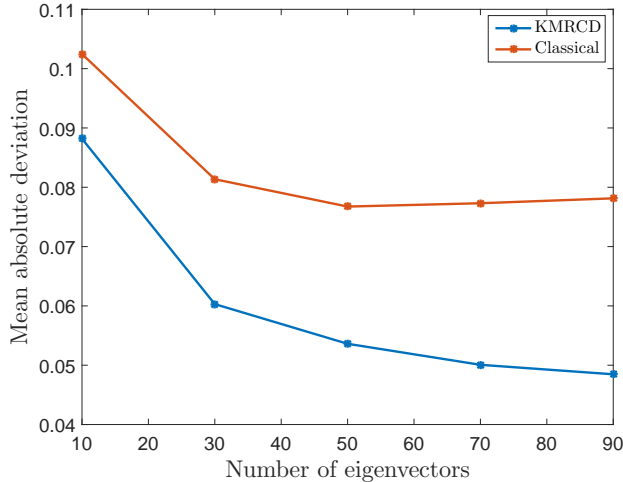


Figure 8: The mean absolute error of the denoised images to the original test images in function of the number of eigenvectors used in the projection. The top curve is for the classical covariance matrix in feature space, the lower curve for KMRCD.

7 Conclusions

The kernel MRCD method introduced in this paper is a robust method that allows to analyze non-elliptical data when used with a nonlinear kernel. Another advantage is that even when using the linear kernel the computation becomes much faster when there are more dimensions than cases, a situation that is quite common nowadays. Due to the built-in regularization the result is always well-conditioned.

The algorithm starts from four kernelized initial estimators, and to each it applies a new kernelized refinement step. The remainder of the algorithm is based on a theorem showing that C-steps in feature space are equivalent to a new type of C-steps on centered kernel matrices, so the latter reduce the objective function. The performance of KMRCD in terms of robustness, accuracy and speed is studied in a simulation, and the method is applied to several examples. Potential future applications of the KMRCD method are as a building block for other multivariate techniques such as robust classification.

Research-level MATLAB code and an example script are freely available from the webpage <http://wis.kuleuven.be/statdatascience/robust/software>.

Acknowledgements. We thank Johan Speybroeck for providing the industrial dataset and Tim Wynants and Doug Reid for their support throughout the project. The research leading to these results has received funding from the European Research Council under the European Union’s Horizon 2020 research and innovation program / ERC Advanced Grant E-DUALITY (787960). This paper reflects only the authors’ views and the Union is not liable for any use that may be made of the contained information. There was also support from the Research Council of KU Leuven (projects C14/18/068 and C16/15/068), the Flemish Government (VLAIO grant HBC.2016.0208 and FWO project GOA4917N on Deep Restricted Kernel Machines), and a PhD/Postdoc grant of the Ford-KU Leuven Research Alliance Project KUL0076 (Stability analysis and performance improvement of deep reinforcement learning algorithms).

References

- [1] Agostinelli, C., Leung, A., Yohai, V.J., Zamar, R.H.: Robust estimation of multivariate location and scatter in the presence of cellwise and casewise contamination. *Test* **24**, 441–461 (2015)
- [2] Alzate, C., Suykens, J.A.K.: Kernel component analysis using an epsilon-insensitive robust loss function. *IEEE Transactions on Neural Networks* **19**, 1583–1598 (2008)
- [3] Boudt, K., Rousseeuw, P.J., Vanduffel, S., Verdonck, T.: The minimum regularized covariance determinant estimator. *Statistics and Computing* **30**, 113–128 (2020)
- [4] Chen, Y., Dang, X., Peng, H., Bart, H.L.: Outlier detection with the kernelized spatial depth function. *IEEE Transactions on Pattern Analysis and Machine Intelligence* **31**, 288–305 (2009)
- [5] Croux, C., Haesbroeck, G.: Influence function and efficiency of the minimum covariance determinant scatter matrix estimator. *Journal of Multivariate Analysis* **71**, 161–190 (1999)
- [6] De Ketelaere, B., Hubert, M., Raymaekers, J., Rousseeuw, P.J., Vranckx, I.: Real-time outlier detection for large datasets by RT-DetMCD. *Chemometrics and Intelligent Laboratory Systems* **199**, 103957 (2020)
- [7] Debruyne, M., Hubert, M., Van Horebeek, J.: Detecting influential observations in kernel PCA. *Computational Statistics & Data Analysis* **54**, 3007–3019 (2010)
- [8] Debruyne, M., Serneels, S., Verdonck, T.: Robustified least squares support vector classification. *Journal of Chemometrics* **23**, 479–486 (2009)
- [9] Debruyne, M., Verdonck, T.: Robust kernel principal component analysis and classification. *Advances in Data Analysis and Classification* **4**, 151–167 (2010)
- [10] Dolia, A.N., De Bie, T., Harris, C.J., Shawe-Taylor, J., Titterton, D.M.: The minimum volume covering ellipsoid estimation in kernel-defined feature spaces. In: *European Conference on Machine Learning*, pp. 630–637. Springer (2006)
- [11] Dolia, A.N., Harris, C.J., Shawe-Taylor, J., Titterton, D.M.: Kernel ellipsoidal trimming. *Computational Statistics & Data Analysis* **52**, 309–324 (2007)
- [12] Donoho, D.L.: Breakdown properties of multivariate location estimators. Tech. rep., Harvard University, Boston (1982)
- [13] Gretton, A., Borgwardt, K.M., Rasch, M.J., Schölkopf, B., Smola, A.: A kernel two-sample test. *The Journal of Machine Learning Research* **13**, 723–773 (2012)
- [14] Haasdonk, B., Pekalska, E.: Classification with kernel mahalanobis distance classifiers. In: *Advances in Data Analysis, Data Handling and Business Intelligence*, pp. 351–361. Springer (2009)
- [15] Hubert, M., Debruyne, M., Rousseeuw, P.J.: Minimum Covariance Determinant and extensions. *Wiley Interdisciplinary Reviews: Computational Statistics* **10**(3), e1421 (2018). DOI 10.1002/wics.1421

- [16] Hubert, M., Rousseeuw, P., Van Aelst, S.: High breakdown robust multivariate methods. *Statistical Science* **23**, 92–119 (2008)
- [17] Hubert, M., Rousseeuw, P.J., Verdonck, T.: A deterministic algorithm for robust location and scatter. *Journal of Computational and Graphical Statistics* **21**, 618–637 (2012)
- [18] Maronna, R.A., Zamar, R.H.: Robust estimates of location and dispersion for high-dimensional datasets. *Technometrics* **44**, 307–317 (2002)
- [19] Mika, S., Schölkopf, B., Smola, A.J., Müller, K.R., Scholz, M., Rätsch, G.: Kernel PCA and denoising in feature spaces. In: *Advances in neural information processing systems*, pp. 536–542 (1999)
- [20] Nelsen, R.B.: *An introduction to copulas*. Springer Science & Business Media (2007)
- [21] Rousseeuw, P.J.: Least median of squares regression. *Journal of the American Statistical Association* **79**, 871–880 (1984)
- [22] Rousseeuw, P.J.: Multivariate estimation with high breakdown point. In: W. Grossmann, G. Pflug, I. Vincze, W. Wertz (eds.) *Mathematical Statistics and Applications*, pp. 283–297. Reidel (1985)
- [23] Rousseeuw, P.J., Croux, C.: Alternatives to the median absolute deviation. *Journal of the American Statistical Association* **88**, 1273–1283 (1993)
- [24] Rousseeuw, P.J., Leroy, A.: *Robust Regression and Outlier Detection*. Wiley-Interscience, New York (1987)
- [25] Rousseeuw, P.J., Raymaekers, J., Hubert, M.: A measure of directional outlyingness with applications to image data and video. *Journal of Computational and Graphical Statistics* **27**, 345–359 (2018)
- [26] Rousseeuw, P.J., Van Driessen, K.: A fast algorithm for the minimum covariance determinant estimator. *Technometrics* **41**, 212–223 (1999)
- [27] Schölkopf, B., Smola, A., Müller, K.R.: Nonlinear component analysis as a kernel eigenvalue problem. *Neural Computation* **10**, 1299–1319 (1998)
- [28] Schölkopf, B., Smola, A.J., Bach, F., et al.: *Learning with kernels: support vector machines, regularization, optimization, and beyond*. MIT press (2002)
- [29] Stahel, W.: Breakdown of covariance estimators. Tech. rep., Fachgruppe für Statistik, ETH Zürich (1981)
- [30] Suykens, J.A.K., Van Gestel, T., De Brabanter, J., De Moor, B., Vandewalle, J.: *Least Squares Support Vector Machines*. World Scientific (2002)
- [31] Vardi, Y., Zhang, C.H.: The multivariate L_1 -median and associated data depth. *Proceedings of the National Academy of Sciences* **97**, 1423–1426 (2000)
- [32] Visuri, S., Koivunen, V., Oja, H.: Sign and rank covariance matrices. *Journal of Statistical Planning and Inference* **91**, 557–575 (2000)

A Supplementary Material

A.1 Algorithms

Algorithms 2 to 5 below describe the initial estimators used. Algorithm 6 carries out the subsequent refinement procedure.

Algorithm 2 Spatial median initial estimator

1. **Input:** kernel matrix K and the number h .
2. Initialize the vector $\gamma = (1/n, 1/n, \dots, 1/n)^\top$ with length n .
3. For iteration = 1 to 10 do
 - (a) Update the coefficients γ_i by

$$\gamma_{\text{new},i} := (K_{ii} - 2\gamma_{\text{old}}^T K_{\cdot i} + \gamma_{\text{old}}^T K \gamma_{\text{old}})^{-\frac{1}{2}}$$

where K_{ii} is the i -th diagonal element of K and $K_{\cdot i}$ is the i -th column of K .

- (b) Normalize $\gamma_{\text{new}} \leftarrow \gamma_{\text{new}} / (\sum_{i=1}^n \gamma_{\text{new},i})$.
 4. Compute the distance of each observation to the spatial median by (6).
 5. Construct H as the set of the h observations with the lowest distances.
 6. Determine the weights w_i using (7).
 7. **Return:** the location weights w_i and the covariance weights $u_i := w_i$.
-

Algorithm 3 Stahel-Donoho initial estimator

1. **Input:** kernel matrix K and the number h .
 2. Initialize the vector of outlyingness values of the n observations as $\eta = (0, \dots, 0)^\top$.
 3. For $q = 1 : 500$ (number of directions) do
 - (a) Select indices $i \neq j$ at random from $\{1, \dots, n\}$
 - (b) Initialize the vector $\lambda = (0, \dots, 0)$ of length n and set $\lambda(i) = +1$ and $\lambda(j) = -1$. This vector represents the direction in \mathcal{F} formed by two observations.
 - (c) Compute the projections of all n points on this direction as $a = K\lambda/\sqrt{\lambda^\top K\lambda}$.
 - (d) Compute the outlyingness of all n projected points as $r^{sd} = |a - \text{median}(a)|/\text{mad}(a)$, where $\text{mad}(\cdot)$ is the median absolute deviation.
 - (e) Update the maximum outlyingness of each observation: $\eta_i^{\text{new}} = \max(\eta_i^{\text{old}}, r_i^d)$.
 4. Define H as the set of h observations with the lowest η_i .
 5. Determine the weights w_i using (7).
 6. **Return:** the location weights w_i and the covariance weights $u_i := w_i$.
-

Algorithm 4 Spatial rank initial estimator

1. **Input:** kernel matrix K and the number h .
 2. Initialize the vector with the n spatial ranks as $R = (0, \dots, 0)^\top$.
 3. Compute the spatial rank R_i of each observation using (10).
 4. Define H as the set of h observations with the lowest values of R_i .
 5. Determine the weights w_i using (7).
 6. **Return:** the location weights w_i and the covariance weights $u_i := w_i$.
-

Algorithm 5 Spatial sign covariance matrix initial estimator

1. **Input:** kernel matrix K .
 2. Compute the spatial median $m_{\mathcal{F}} = \sum_{i=1}^N \gamma_i \phi(x_i)$ using Algorithm 2.
 3. The location weights are taken as $w_i = \gamma_i$.
 4. Compute the distances $\|\phi(x_i) - m_{\mathcal{F}}\|$ to the spatial median from (6). The covariance weights are then computed as $u_i = 1/\|\phi(x_i) - m_{\mathcal{F}}\|$.
 5. **Return:** the location weights w_i and the covariance weights u_i .
-

Algorithm 6 Refinement of initial estimators

1. **Input:** kernel matrix K and number h , weights w_i to determine the initial estimate of location $c_{\mathcal{F}}$ by (8) and weights u_i to compute the initial estimate of scatter $\hat{\Sigma}_{\mathcal{F}}$ by (9).
 2. Project the data on the eigenvectors of $\hat{\Sigma}_{\mathcal{F}}$ using (11).
 3. Compute the spatial median of the adjusted kernel matrix (12) using Algorithm 2, which gives the weights γ^* .
 4. Determine the distance $d_{\mathcal{F}}^*(x)$ of each observation by (13).
 5. Define H as the set of h observations with the lowest distance.
 6. **Output:** the refined subset H .
-

A.2 The special case of the linear kernel

Given an $n \times p$ matrix X of observations, its regularized covariance matrix is given by

$$\hat{\Sigma}_{\text{reg}} = (1 - \rho)\hat{\Sigma}_{\mathcal{F}} + \rho I_{\mathcal{F}} = \frac{1 - \rho}{n - 1} \tilde{\Phi} \tilde{\Phi}^{\top} + \rho I_{\mathcal{F}} .$$

The regularized kernel matrix is defined as

$$\tilde{K}_{\text{reg}} = (1 - \rho)\tilde{K} + (n - 1)\rho I_n = (1 - \rho)\tilde{\Phi}^{\top} \tilde{\Phi} + (n - 1)\rho I_n .$$

For the linear kernel, the eigenvectors of the covariance matrix are given by

$$v_{\mathcal{X}}^k = \sum_{i=1}^n (v_{\mathcal{F}}^k)_i (x_i - c_{\mathcal{F}}) ,$$

where $c_{\mathcal{F}} = \frac{1}{n} \sum_{i=1}^n x_i$ and $(v_{\mathcal{F}}^k)_i$ is the i -th element of the k -th eigenvector of the centered kernel matrix. We can now write $\hat{\Sigma}_{\mathcal{F}}$ using the eigenvectors of the kernel matrix:

$$\hat{\Sigma}_{\mathcal{F}} = V^{\top} \Lambda V = \frac{1}{n - 1} \tilde{X}^{\top} \tilde{V}_{\mathcal{F}} \Lambda \tilde{V}_{\mathcal{F}}^{\top} \tilde{X} ,$$

where the $n \times n$ matrix $\tilde{V}_{\mathcal{F}} = [v_1/\sqrt{\lambda_1}, \dots, v_n/\sqrt{\lambda_n}]$ contains the normalized eigenvectors of the centered kernel matrix and \tilde{X} is the centered data matrix. The regularized covariance matrix is thus equal to

$$\hat{\Sigma}_{\text{reg}} = \frac{1 - \rho}{n - 1} \tilde{X}^{\top} \tilde{V}_{\mathcal{F}} \Lambda \tilde{V}_{\mathcal{F}}^{\top} \tilde{X} + \rho I_n .$$

A.3 Effect of the imposed condition number

The main text considers the condition number κ of a covariance matrix in two different places. The first occurrence is in the KMRC algorithm itself. Indeed, the choice of the regularization parameter ρ in (4) must be such that the condition number $\kappa(\rho)$ given by (14) is at most 50. The second occurrence is in the simulation study with linear kernel, when in each replication a random correlation matrix Σ of type ALYZ is generated according to Section 4 of [1], who impose that such correlation matrices have condition number $\kappa(\text{ALYZ}) = 100$.

It is natural to wonder about the effect of both choices, and to what extent they interact. To study this we repeat part of the simulation of Section 5.1, for the hardest settings with (n, p) set to $(400, 200)$ and $(200, 400)$ and with ε equal to 0 and 0.3 and $h = 0.5$. The contamination types are as before. We now allow the condition number $\kappa(\text{ALYZ})$ to be 100, 300 and 1000. The imposed condition number $\kappa(\rho)$ in the algorithm can now take the values 50, 100 and 1000. The averaged KL divergence over 100 replications is shown in Table 4.

Table 4: The KL divergence in function of the condition number of the ALYZ covariance matrix $\kappa(\text{ALYZ})$ and $\kappa(\rho)$ of the KMRC algorithm with $h = 0.5$.

		Point contamination			Shift contamination			Cluster contamination		
		Value of $\kappa(\text{ALYZ})$			Value of $\kappa(\text{ALYZ})$			Value of $\kappa(\text{ALYZ})$		
		100	300	1000	100	300	1000	100	300	1000
$\varepsilon = 0$:										
400×200	$\kappa(\rho) = 50$	127	146	197	128	147	198	127	145	197
	$\kappa(\rho) = 100$	158	166	196	159	166	197	159	167	194
	$\kappa(\rho) = 1000$	269	264	265	268	265	264	268	264	264
200×400	$\kappa(\rho) = 50$	674	761	969	677	759	969	675	759	943
	$\kappa(\rho) = 100$	1104	1168	1340	1108	1169	1326	1107	1169	1323
	$\kappa(\rho) = 1000$	6480	6380	6401	6492	6366	6367	6440	6375	6403
$\varepsilon = 0.3$:										
400×200	$\kappa(\rho) = 50$	125	142	11536	125	143	205	125	144	251
	$\kappa(\rho) = 100$	156	163	20581	155	164	193	155	164	422
	$\kappa(\rho) = 1000$	265	10189	84460	256	185	209	257	189	209
200×400	$\kappa(\rho) = 50$	694	776	13729	692	786	1007	693	771	1041
	$\kappa(\rho) = 100$	1138	1199	25464	1157	1216	1416	1152	1213	1344
	$\kappa(\rho) = 1000$	6766	72332	195728	6906	1570	5405	6862	1568	5275

Comparing the choices of $\kappa(\rho)$, we observe that the strongest regularization ($\kappa(\rho) = 50$) consistently performed best (had the lowest KL), across all scenarios considered. That is, even when the true $\kappa(\text{ALYZ})$ is substantially above 50, setting $\kappa(\rho)$ to 50 did better or equally well than setting it to 100 or 1000. This provides some support for the choice $\kappa(\rho) = 50$ in the KMRC algorithm.

A.4 Comparison of initial estimators

In this section we study the computation time and the performance of the four initial estimators used by KMRCDC, in several scenarios:

1. as in the simulation with linear kernel (Section 5.1), with point contamination, $\varepsilon = 0.3$, $h = 0.5$, and $(n, p) = (400, 200)$;
2. as in the first setting, but now with $(n, p) = (200, 400)$ so there are more variables than cases;
3. the t -copula setting of the simulation with nonlinear kernels, as in Figure 4 of section 5.2, with $\varepsilon = 0.2$ and $h = 0.75$.
4. the circle-based setting of the simulation with nonlinear kernels, as in Figure 5, also with $\varepsilon = 0.2$ and $h = 0.75$.

Each setting is replicated 100 times, and in each replication we monitor the computation time of the individual initial estimators as well as the time needed by the subsequent C-steps procedure. The averaged computation times (in seconds) are given in Table 5.

Table 5: Averaged computation times of the four initial estimators (init) and the subsequent C-steps, in the four data settings described in Section A.4.

	Spatial median		SDO		Spatial rank		SSCM	
	init	C-steps	init	C-steps	init	C-steps	init	C-steps
Setting 1	0.020	0.002	0.046	0.002	0.406	0.002	0.034	0.002
Setting 2	0.007	0.001	0.029	0.001	0.070	0.001	0.010	0.001
Setting 3	0.024	0.024	0.055	0.024	0.667	0.025	0.037	0.024
Setting 4	0.023	0.018	0.052	0.028	0.670	0.027	0.035	0.034

In Table 5 we see that the C-steps never take longer than their initial estimator, and that the computation times of the C-steps are similar across the four initial estimates. Among the initial estimators, the spatial rank took the longest, whereas the other three took about the same time. Also note that the bivariate settings 3 and 4 are not faster than setting 1 because their sample size is $n = 500$, so the computations are done on kernel matrices of size 500×500 .

We also counted the number of times each initial estimator provided the best solution (i.e. the lowest covariance determinant) after its C-steps converged. The results are given in Table 6. Note that two or more estimators can give the same best solution, so the row sums can exceed 100. In settings 1 and 2 of high-dimensional data analyzed with the linear kernel, the SSCM initial estimator outperformed the others. In settings 3 and 4 with nonlinear kernels, all four initial estimators performed about equally well.

Table 6: The number of times each initial estimator provided the best solution (i.e. the lowest covariance determinant) after C-steps, for the 4 settings in Table 5.

	Spatial median	SDO	Spatial rank	SSCM
Setting 1	4	0	1	95
Setting 2	0	5	0	95
Setting 3	57	65	52	66
Setting 4	52	60	58	53

A.5 Additional simulation results with linear kernel

Table 7 shows the mean squared error (MSE) of the estimates $\hat{\Sigma}$ in the same setup as Table 1 of the main text. For readability the MSE values are multiplied by 1000. Table 8 lists the average values of the regularization parameter ρ in each setting.

Table 7: MSE for Σ of type ALYZ (multiplied by 1000).

	Point contamination			Shift contamination			Cluster contamination		
	Value of h/n			Value of h/n			Value of h/n		
	0.50	0.75	0.90	0.50	0.75	0.90	0.50	0.75	0.90
$\varepsilon = 0 :$									
KMRCD									
400×200	4.31	2.96	2.47	4.33	2.94	2.46	4.35	2.94	2.43
300×200	5.51	3.81	3.19	5.44	3.80	3.18	5.52	3.79	3.21
200×200	7.88	5.47	4.66	7.78	5.54	4.71	7.77	5.42	4.71
200×300	7.36	5.21	4.45	7.29	5.21	4.45	7.37	5.22	4.45
200×400	6.95	5.04	4.32	6.91	4.99	4.31	6.94	5.11	4.29
MRCD									
400×200	4.32	2.99	2.51	4.32	2.96	2.51	4.34	2.99	2.48
300×200	5.59	3.83	3.22	5.51	3.83	3.21	5.54	3.83	3.26
200×200	7.89	5.60	4.67	7.85	5.59	4.69	7.75	5.61	4.70
200×300	7.42	5.28	4.51	7.42	5.28	4.49	7.47	5.33	4.52
200×400	7.04	5.04	4.33	7.08	5.04	4.36	7.01	5.09	4.31
$\varepsilon = 0.1 :$									
KMRCD									
400×200	4.35	2.99	2.53	4.38	3.00	2.51	4.37	2.99	2.50
300×200	5.61	3.86	3.29	5.59	3.90	3.28	5.60	3.89	3.27
200×200	7.97	5.60	4.86	7.93	5.58	4.84	7.99	5.64	4.83
200×300	7.38	5.31	4.59	7.44	5.32	4.56	7.39	5.30	4.60
200×400	7.09	5.13	4.39	7.03	5.11	4.41	7.04	5.10	4.43
MRCD									
400×200	4.43	3.05	2.58	4.52	3.12	2.60	4.49	3.11	2.59
300×200	5.75	3.95	3.34	5.85	4.05	3.35	5.88	4.04	3.36
200×200	8.33	5.74	4.94	8.18	5.81	4.97	8.20	5.86	4.96
200×300	7.68	5.45	4.62	7.78	5.57	4.69	7.78	5.52	4.72
200×400	7.22	5.15	4.38	7.44	5.28	4.52	7.41	5.31	4.55
$\varepsilon = 0.3 :$									
KMRCD									
400×200	4.55	247.32	58.13	4.55	18.74	40.78	4.54	18.75	39.88
300×200	5.80	242.03	58.59	5.88	18.34	38.22	5.80	18.47	39.34
200×200	8.28	246.56	59.43	8.51	19.15	37.54	8.37	19.09	37.85
200×300	7.78	109.01	26.17	7.88	9.43	16.42	7.87	9.43	16.47
200×400	7.41	61.23	15.02	7.40	6.08	9.44	7.45	6.13	9.49
MRCD									
400×200	4.16	329.39	89.32	4.85	37.14	115.04	4.87	36.75	114.14
300×200	5.25	312.86	90.28	6.39	37.43	109.50	6.31	37.72	114.09
200×200	7.44	326.92	92.79	9.07	38.99	108.50	8.83	39.07	110.41
200×300	6.49	128.66	33.82	8.52	17.44	42.28	8.56	17.53	42.15
200×400	5.62	64.31	16.70	7.97	10.51	21.52	8.03	10.75	21.83

Table 8: Regularization coefficients for Σ of type ALYZ.

	Point contamination			Shift contamination			Cluster contamination		
	Value of h/n			Value of h/n			Value of h/n		
	0.50	0.75	0.90	0.50	0.75	0.90	0.50	0.75	0.90
$\varepsilon = 0 :$									
KMRCD									
400×200	0.091	0.075	0.069	0.093	0.073	0.071	0.088	0.077	0.072
300×200	0.094	0.086	0.079	0.097	0.089	0.079	0.097	0.088	0.087
200×200	0.117	0.096	0.091	0.119	0.100	0.091	0.117	0.098	0.092
200×300	0.155	0.116	0.107	0.155	0.116	0.109	0.162	0.116	0.108
200×400	0.179	0.143	0.125	0.178	0.139	0.124	0.178	0.138	0.126
MRCD									
400×200	0.091	0.073	0.063	0.093	0.070	0.064	0.092	0.073	0.064
300×200	0.100	0.084	0.078	0.098	0.087	0.075	0.099	0.085	0.077
200×200	0.115	0.099	0.094	0.115	0.102	0.094	0.115	0.102	0.092
200×300	0.143	0.116	0.107	0.140	0.119	0.108	0.145	0.117	0.107
200×400	0.164	0.139	0.125	0.169	0.138	0.125	0.165	0.134	0.124
$\varepsilon = 0.1 :$									
KMRCD									
400×200	0.089	0.079	0.074	0.089	0.076	0.074	0.095	0.080	0.069
300×200	0.098	0.085	0.079	0.097	0.089	0.083	0.098	0.088	0.079
200×200	0.424	0.098	0.097	0.120	0.099	0.090	0.120	0.098	0.092
200×300	0.156	0.120	0.110	0.153	0.118	0.112	0.150	0.118	0.112
200×400	0.181	0.139	0.127	0.176	0.140	0.126	0.176	0.140	0.125
MRCD									
400×200	0.087	0.073	0.064	0.082	0.061	0.059	0.081	0.065	0.054
300×200	0.096	0.081	0.073	0.092	0.076	0.069	0.089	0.073	0.065
200×200	0.115	0.096	0.091	0.102	0.088	0.078	0.103	0.088	0.081
200×300	0.146	0.118	0.109	0.133	0.105	0.098	0.129	0.107	0.100
200×400	0.172	0.138	0.130	0.153	0.125	0.115	0.154	0.124	0.114
$\varepsilon = 0.3 :$									
KMRCD									
400×200	0.094	0.524	0.740	0.097	0.507	0.733	0.091	0.517	0.744
300×200	0.100	0.505	0.738	0.101	0.527	0.746	0.101	0.521	0.742
200×200	0.124	0.507	0.746	0.119	0.511	0.749	0.118	0.521	0.745
200×300	0.151	0.508	0.749	0.153	0.516	0.748	0.155	0.504	0.748
200×400	0.178	0.512	0.740	0.175	0.510	0.737	0.174	0.518	0.748
MRCD									
400×200	0.534	0.644	0.705	0.071	0.308	0.541	0.068	0.314	0.555
300×200	0.459	0.745	0.724	0.078	0.325	0.557	0.080	0.323	0.558
200×200	0.750	0.688	0.712	0.092	0.319	0.565	0.089	0.326	0.564
200×300	0.774	0.770	0.760	0.116	0.349	0.591	0.118	0.338	0.592
200×400	0.796	0.790	0.775	0.139	0.364	0.610	0.142	0.372	0.616

A.6 Additional figures for non-elliptical data

Here we illustrate the Frank, Clayton, and Gumbel copulas [20] with Kendall rank correlation $\tau = 0.6$. Figure 9 below is analogous to Figure 4 for the t copula in the main text.

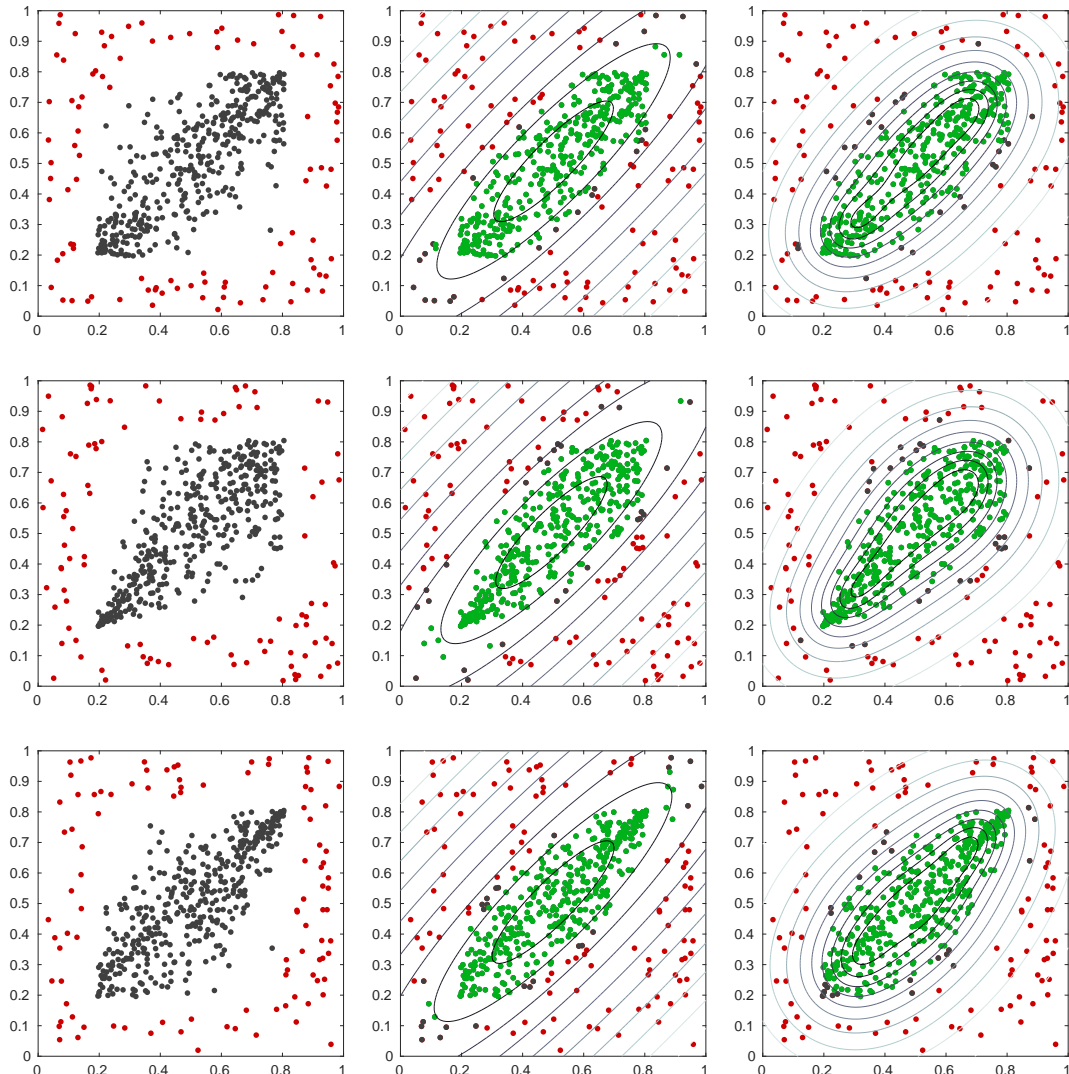


Figure 9: Illustration of the non-elliptical simulation setting, on data sets generated from the Frank (top), Clayton (middle), and Gumbel (bottom) copulas. Each dataset contains 20% of outlying observations. In the left panels, the regular observations are shown in black and the outliers in red. The results of the MRCD estimator are in the middle panels, and those of the KMRC estimator in the rightmost panels, each for $h = 0.75n$. In those panels the points in the h -subset are shown in green, and the other points with the $n(1 - \varepsilon)$ lowest (kernel) Mahalanobis distance are depicted in grey. The remaining points are shown in red. The curves are contours of the robust (kernel) Mahalanobis distance.